ADVANCES IN MATERIALS SCIENCE, Vol. 26, No. 1 (87), March 2026

DOI: 10.2478/adms-2026-0002

**Ayesha Kausar***

*National Center For Physics, Quaid-i-Azam University Campus, Islamabad, Pakistan*

** dr.ayeshakausar@yahoo.com*

# NON-COVALENTLY INTERACTED THERMOSETTING/CONDUCTING MATRICES AND FULLERENE DERIVED NANOCOMPOSITES - DESIGN, FEATURES AND TECHNOLOGICAL APPLICATIONS

ABSTRACT

This comprehensive review highlights two important categories of fullerene reinforced nanocomposites (thermosetting/fullerene and conductive/fullerene) having physical/non-covalent interlinkings (electrostatic, hydrogen bonding and π-π aromatic ring stackings) in macromolecular-nanofiller phases. As per literature, physical linkages of macromolecular matrices with fullerene nano-additives caused substantial enhancements in morphological, mechanical, thermal, dielectric, tribological, electrochemical, anticorrosion, photovoltaic, power energy conversion, capacitive and other properties of ensuing thermosets/fullerene and conductive/fullerene hybrids. Accordingly, non-covalent interactions effectively increased structural stability/performance of polymer/fullerene nanocomposites via homogeneous macromolecular chain orientations and miscibility effects along with uniform nanoparticle dispersions and compatible interfaces. Particularly, initial section 2 (after introduction) explains basics of fullerene and Section 3 essentially describes dispersion state, interfacial aspects, and property-performance profiles, and mechanism of physically linked polymer/fullerene nanocomposites. Next, section 4 portrays literature state of thermosets/fullerene nanocomposites. Mostly, non-covalent nanocomposites diglycidyl ether of bisphenol A epoxy/blends with fullerene were processed via sonication, in situ, solution, and curing techniques. Herein, adding fullerene notably enhanced tensile strength, modulus, toughness, dielectric constant, and anticorrosion potential of epoxies by ~ 80-100 %. For bulk heterojunction solar cells, epoxy/fullerene hybrids depicted power conversion efficiency of > 3 %. Next, section 5 speaks to conductive (polyaniline, polypyrrole, polythiophene derivatives) nanocomposites with fullerene, mostly synthesized by in situ, solution/sonication methods. In photovoltaics, conducting polymer/fullerene nanocomposites had superior power conversion efficiency of 30 % and for supercapacitors/batteries specific capacitance and capacity retention were > 800 $Fg^{-1}$ and > 90 %, respectively. Incidentally, last section states prospective future and conclusive remarks on thermoset/fullerene and conductive/fullerene nanomaterials. Hence, objective of this review is to unfold practical amplification of non-covalently interlinked thermosetting/fullerene and conductive/fullerene nanocomposites (high-tech anticorrosion coatings, solar cells, rechargeable batteries) for concerned field researchers. Nevertheless, physically interlinked polymer/fullerene nanocomposites face various challenges of macromolecular chain aggregations, non-uniform dispersions, and uncontrolled processing parameters, thereby affecting microstructures and property-performance contours.

***Keywords:*** *Fullerene; macromolecules; nanocomposites, physical interactions; epoxy; conductive polymers; coatings; solar cells*

## INTRODUCTION

Thermosetting polymers or thermosets, for instance, epoxies, phenolics, polyesters and polyurethanes, are high molecular weight macromolecules having irreversible crosslinking between their main chains [1]. Another important type of polymers is the conducting or conjugated polymers, for example polyaniline, polypyrrole and polythiophene, which are

*Received: 20.10.2025; Received in revised form: 18.01.2026; Accepted: 11.02.2026*

usually characterized by their aromatic main chain conjugation and unique semiconducting properties. As a polymeric nano-reinforcement nanostructure, fullerene is a unique zero dimensional nano-allotrope of carbon having a hollow cage like nanostructure [2]. Similar to other carbonaceous nanoparticles, such as graphene, nanodiamonds or carbon nanotubes, fullerene has been considered as an effective nano-additive for the thermosetting as well as conductive macromolecular matrices to form the high performance nanomaterials [3]. Successively, the literature hitherto reported on the synthesis, valuable characteristics and practical applications of the advanced thermosetting/fullerene [4, 5] and conjugated polymer/fullerene [6, 7] nanomaterials. In this context, nature and role of non-covalent interactions, like van der Waals, π-π stacking, electrostatic and hydrogen bindings, for an effective macromolecular-nanofiller interface formation, facile processing and advanced physical characteristics of the polymer/fullerene hybrids have been essentially investigated in the literature [8-10]. Besides, a few efficiently designed non-covalently associated polymer/fullerene nanocomposite systems have been reported valuable for coatings and devices related applications [11].

This novel state-of-the-art overview debates current scientific state of the physically/non-covalently interlinked thermoset/fullerene and conjugated polymer/fullerene nanomaterials, which, to the best of the knowledge, has not been priorly reviewed in the literature available up till now. For a better comprehension, Fig. 1 shows an overall schematic diagram with section wise division (fundamentals, nanocomposite categories, applications) and layout of the current review.

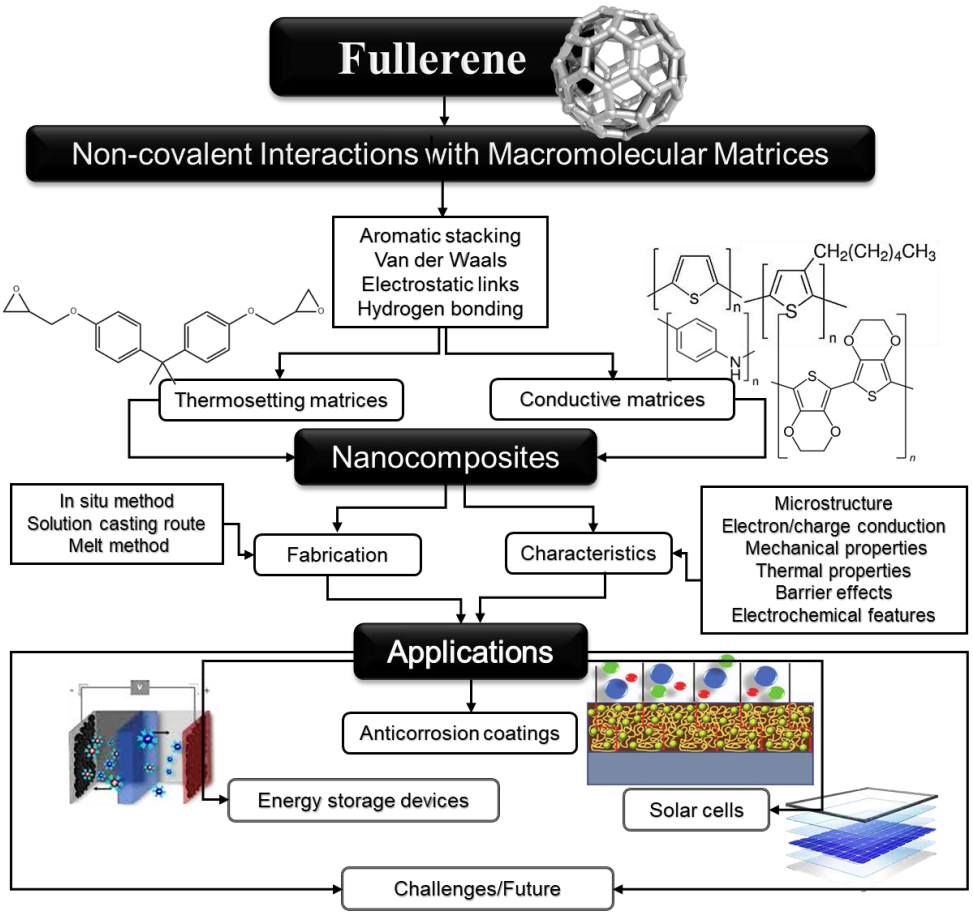


**Fig. 1**. A schematic diagram showing layout of the current literature review

According to the literature investigations, the physical interactions in the polymer/fullerene nanocomposites played a key role for controlling the microstructural, electrical conductivity, thermal stability, thermal conductivity and immeasurable allied physical properties of these hybrids. Subsequently, development and effectiveness of the non-covalent linkages between polymer/fullerene seemed to be dependent upon various factor, like type, molecular weight and miscibility of the macromolecular matrix as well as nanofiller surface functionalization and its contents, related to the polymers and the nanofillers. Consequently, non-covalent interactions may affect the design, processing, interfacial aspects and so the resulting characteristics of the fullerene filled thermosetting or conductive macromolecular matrices. Henceforward, the ensuing polymer/fullerene nanomaterials revealed valuable morphological, electrical, thermal, mechanical, barrier and allied physical features for their technical applications in the fields of anticorrosion coatings and solar cells/batteries. Nevertheless, future advancements in the field of physically interlinked polymer/fullerene nanomaterials depend upon the design of new functional fullerene molecules, functional macromolecular matrices and advanced fabrication approaches (having optimum processing conditions) to overcome the underlying property-processing encounters for the manufacturing of high-tech industrial level nanostructures.

## FULLERENE

Among zero dimensional nanocarbons, fullerene, nanodiamond, carbon nanoonion, carbon dots or graphene quantum dots have been developed and explored so far by the field researchers [12]. Table 1 shows comparative properties of few important zero dimensional carbon nanomaterials. Particularly, fullerene is a hollow spherical nano-entity which is made up of hexagonally arranged $sp^2$ hybridized carbon atoms in its structure [13]. Fullerene molecule was initially discovered in 1985 and was found to be composed of pentagonal and hexagonal rings in its cage like sphere-shaped nanostructure [14]. Fullerene molecule can be imagined as a round enfolded graphene nanosheet, forming a ball like structure, with aromatic conjugation in its nanostructure [15]. Fullerene exists in various molecular sizes, like $C_{20}$ $C_{28,}$ $C_{30,}$ $C_{60}$, $C_{70,}$ $C_{120}$ and so on, depending upon the number of carbon atoms in its ring [16]. Among these fullerene analogues, $C_{60}$, also known as Buckminster fullerene, is one the most symmetrical forms of these zero dimensional molecules [17]. Consequently, fullerene $C_{60}$ has been widely investigated in the literature, owing to its unique structure and characteristics [18]. In this regard, various effective techniques have been utilized to synthesize the fullerene molecules including nano-cutting method, chemical vapor deposition, laser/plasma tactics, arc discharge practices, plasma processes and organic synthesis approaches [19]. Owing to valuable optical, electronic, heat/electrical conduction, thermal stability, mechanical stability and chemical reactivity characteristics, the resulting fullerene molecules have been analyzed for technical applications in the photovoltaics, batteries, capacitors and sensing devices [20]. Besides, fullerene molecules have been used as efficient carbonaceous nonreinforcements for polymers.

***Table 1.*** *Properties of few significant zero dimensional nanomaterials*

| Zero dimensional nanoparticles | Discovery | Structure | Synthesis | Surface area | Properties | Ref |
|---|---|---|---|---|---|---|
| Nanodiamonds | 1963 | $Sp^3$ hybridized carbon atoms; hexagonal/cubic diamond lattices; size 5-100 nm | Detonation; carbon soot; high temperature and pressure 2000 °C & 200 GPa, respectively | 300-400 sq.m $g^{-1}$ | Electrical conductivity 3.4 × $10^{-7}$ $Ohm^{-1}$ $cm^{-1}$) (10-20 % increase with temperature) florescence wavelength > 690 nm; lubrication | 21 |
| Fullerene | Kroto, 1985 | Hollow cages; $sp^2$ hybridized carbon atoms; pentagons & hexagons; symmetrical; $C_{60}$ external diameter ~ 0.71 nm; different types as per number of carbon atoms | Graphite vaporization; plasma discharge; laser ablation; hydrocarbon pyrolysis | 2625 $m^2$ $g^{-1}$ ($C_{60}$) | Electron mobility $10^{-4}$ to $10^{-3}$ $cm^2$ $(V\ s)^{-1}$; thermal stability; tunable band gap; photoluminescence; lubrication; strength; abrasion | 22 |
| Carbon nano-onions | Ugarte, 1992 | Multi-shell fullerene; Not perfectly spherical shape; small nanoparticles 2-8 shells ~ 3-10 nm; Large nanoparticles ~ 25-30 nm | Electron beam irradiation of carbon precursor; arc discharge; Carbon soot heating 2100-2250 °C (vacuum); solution ozonolysis; electrochemical processes | 30-500 $m^2$ $g^{-1}$ | Electrical conductivity 2-4 S $cm^{-1}$ | 23 |
| Carbon Dots | Xu, 2004 | Size few nm to ~ 5-10 nm | Top-down: cutting of carbon nanostructures; acidic oxidation; arc discharge (4000 K); laser ablation method; bottom up: combustion; microwave pyrolysis; microwave; hydrothermal | ~ 1300-1500 $m^2$ $g^{-1}$ | Electrical conductivity; charge transportation; quantum confinement; edge effects; florescence; photoluminescence | 24 |

## INTERACTIONS/DISPERSION FEATURES OF CARBONACEOUS NANOPARTICLES IN MACROMOLECULAR MATRICES

Various types of nanocarbon nanoparticles, like zero dimensional spherical (fullerene, quantum dots), one dimensional tubular (carbon nanotube, carbon nanofiber), two dimensional nanosheet (graphene) and three dimensional network (nanocarbon hydrogel), have been synthesized and explored in the literature so far [25, 26]. According to the research reports, all these carbonaceous nanoparticles own tendencies to be applied as nanofillers in various polymeric matrices, like thermosets, thermoplastics, rubbers or conducting polymers, to form the nanocomposites. In this regard, macromolecular properties, like backbone

structure, molecular weight, amount and solubility, of the matrices seemed to influence the dispersion features of the nanocarbon nanoparticles. Subsequently, the scattering and orientation patterns of these carbonaceous nanoparticles in the polymeric matrices were found to affect the physical property profiles of the resulting nanomaterials [27]. According to the research investigations so far, uniform nanoparticle dispersions have been suggested favorable for the formation of the high performance polymer/nanocarbon nanocomposites [28]. In this concern, optimum molecular weight of the macromolecules has been considered valuable for developing fine matrix-nanofiller interactions for the formation of well-compatible interfaces with the nanofillers; therefore, enhancing the physical characteristics, like conductivity, strength and heat stability, of the resulting nanocomposites. In addition, nanoparticle dispersion can be significantly influenced by the solubility properties and chemical nature of the macromolecular backbone. On the other hand, performance of the polymer/nanocarbon nanocomposites also seemed to be dependent upon the type, amounts and interfacial level interactions of the carbon nanoparticles with the macromolecules [29]. Furthermore, choice of an appropriate fabrication technique has been considered indispensable for uniform dispersion of the carbonaceous nanoparticles in the macromolecular matrices [30]. Convincingly, dispersion patterns and microstructural characteristics of the polymer/nanocarbon nanocomposites seemed to be strongly reliant upon various factors, like macromolecular properties, nanofiller features and the synthesis techniques used for the formation of these nanomaterials [31].

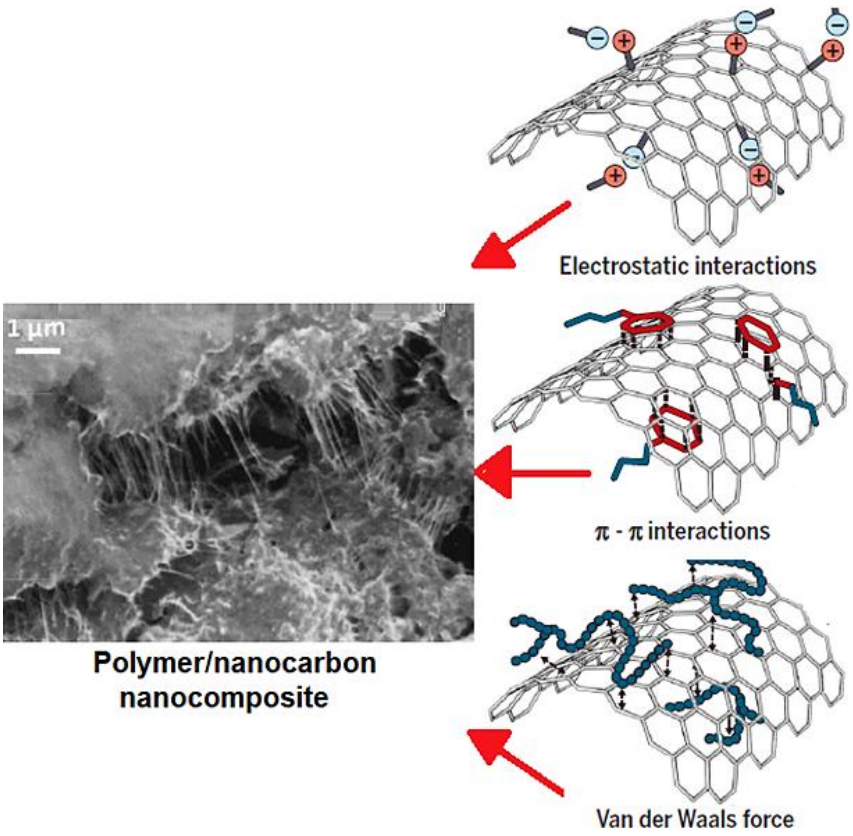


**Fig. 2.** Schematic of interactions in epoxy/nanocarbon nanocomposite: (left) scanning electron microscopy micrograph; (right) mechanisms of possible physical links in matrix-nanofiller [33]. Reproduced with permission from The American Association for the Advancement of Science

Apart from these, according to the literature, an imperative factor for enhancing the nanoparticle dispersion in the macromolecular matrices is the development of physical or

covalent linkages of the functional nanocarbon surfaces with the matrices. Generally speaking, carbonaceous nanoparticles are capable of developing weak van der Waals, electrostatic, ring stacking and hydrogen binding interactions with the base materials [32]. Fig. 2 presents a schematic of possible mechanisms behind physical interactions between polymer and nanocarbon surfaces [33]. Consequently, these physical interactions between the macromolecular matrix-nanofiller may develop strong interfaces, therefore affecting the final property-performance profile of the nanocarbons filled polymeric nanocomposites.

In the literature, the dispersion states of the nanocarbon nanoparticles have been analyzed through structural, microscopic and modeling/theoretical methodologies [34]. It has been observed that uniform nanoparticle dispersions and orderly alignments in the macromolecular matrices resulted in heat/mechanical stability, electrical/thermal conductivity and allied physical properties of the polymer/nanocarbon nanocomposites [35]. Accordingly, significant research endeavors have been noticed for non-covalently reinforced thermosetting and conductive polymers, as surveyed in subsequent review sections.

## CHARACTERISTICS OF NON-COVALENTLY BONDED THERMOSETTING MATRIX/FULLERENE NANOCOMPOSITES

Thermosetting polymer, often called a thermoset, is a polymer having irreversible crosslinking between its backbones which is usually induced by the factors, like heat, radiations, pressure or catalysts during curing process [36]. Epoxy is one of the most commonly developed and investigated form of the thermosetting polymers [37]. Epoxies, like diglycidyl ether of bisphenol-A, diglycidyl ether of bisphenol-F, diglycidyl ether of bisphenol-H or novolac, are usually low molecular weight compounds having epoxide groups in the main chains or chain ends, for example [38]. For hardening purposes, generally, low molecular weight epoxies are used to react with the short chain compounds, like diols, diamines, diisocyanates, etc., in the presence of heat or UV light [39]. Upon hardening, the resulting high molecular weight epoxy resins may have remarkable thermal/mechanical/chemical stability, adhesion, tribological and corrosion resistance features for applications in high performance coatings, adhesives and engineering structures [40]. Like majority of the thermosetting or thermoplastic polymers, epoxies have the capability to form nanocomposites with carbon/inorganic nanoparticle nanoreinforcements [41]. Among carbonaceous nanoparticles, like graphene, carbon nanotubes or nanodiamonds, fullerene molecules have been studied as valuable nanocarbon nano-additives for the epoxy matrices. Essentially, including fullerene nanoparticles in the epoxy/carbon fiber composites have been found to positively affect the mechanical characteristics of the resulting nanomaterials for their technical application in automotive engineering parts [42]. In this regard, including small amounts of fullerene nano-additives in epoxies significantly increased the mechanical strength of the matrices.

Xiang et al. [43], for example, prepared the poly(ethylene oxide)-fullerene using click reactions and then reinforced in the diglycidyl ether of bisphenol A epoxy matrix by solution mixing and curing techniques. Moreover, a poly(ethylene oxide)-block-poly(N-vinylcarbazole) was synthesized through reversible addition-fragmentation chain transfer/macromolecular design for blend formation with the epoxy matrix. For comparative studies, the poly(ethylene oxide)-fullerene nanoparticles were also reinforced in the epoxy/poly(ethylene oxide)-block-poly(N-vinylcarbazole) blends. Fig. 3 A shows a synthesis route for the formation of fullerene $C_{60}$ interlinked poly(ethylene oxide) through azido group

cycloaddition reactions. Figs. 3 B a & b illustrates the transmission electron microscopy micrographs of the epoxy matrix having poly(ethylene oxide)-fullerene contents, of 3 and 6 wt.%, respectively. According to the micrographs, including nano-additives resulted in uniform dispersions and nanodomains formation in epoxy, owing to physical or noncovalent interactions (mainly hydrogen bonding and aromatic ring stackings) between the macromolecular matrix and the poly(ethylene oxide)-fullerene nanoparticles. Nevertheless, increasing the fullerene contents, from 3 and 6 wt.%, did not influence its dispersion patterns or nanodomain formation in the matrix, seemingly due to the matrix-nanofiller compatibility effects.

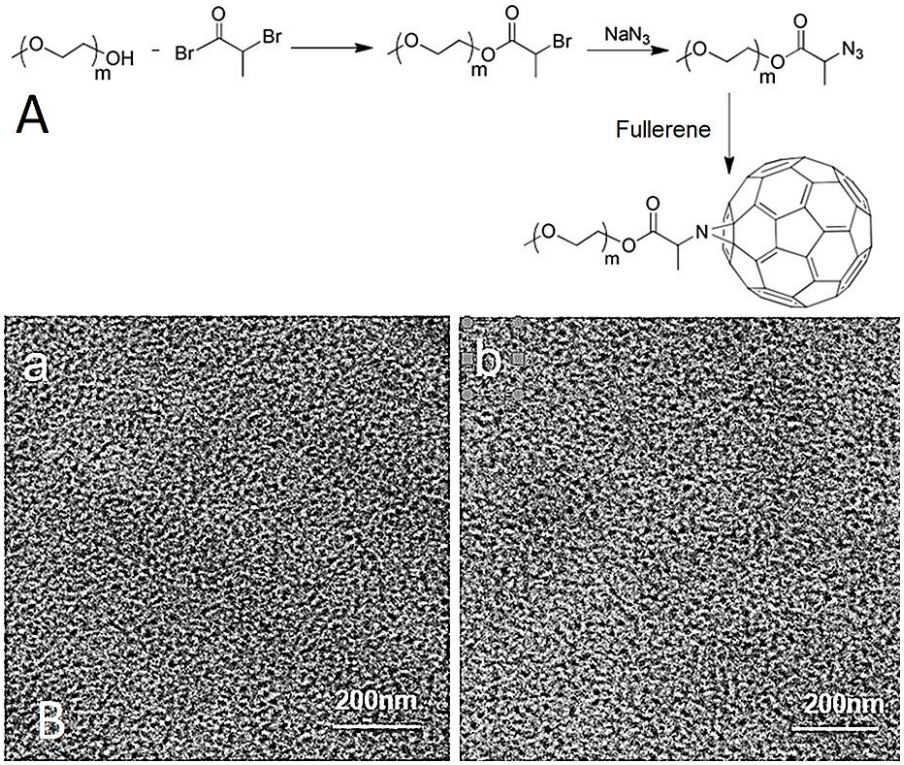


**Fig. 3.** (A) A scheme for the synthesis of poly(ethylene oxide) interlinked fullerene nanocomposite. (B) transmission electron microscopy images of the epoxy containing (a) poly(ethylene oxide)-fullerene with 3 wt.% nanofiller; and (b) poly(ethylene oxide)-fullerene with 6 wt.% nanofiller. Reproduced from [43] with permission from Elsevier

Additionally, the dielectric constant and dielectric loss features of the resulting nanomaterials were studied. Neat epoxy had dielectric constant, of 3.7 at $10^3$ Hz, which was slightly increased to 4.2 with the addition, of 12 wt. %, poly(ethylene oxide), due to higher dipole density of the binary blends, relative to the pristine epoxy (Fig. 4 A). Contrarily, the dielectric loss values of the epoxy/poly(ethylene oxide) blends seemed to be declined with the increasing poly(ethylene oxide) contents in the epoxy matrix, probably due to the intermolecular hydrogen bonding interactions between the epoxy and the poly(ethylene oxide) phases. In the case of the epoxy/poly(ethylene oxide)-block-poly(N-vinylcarbazole) blend, including poly(ethylene oxide)-block-poly(N-vinylcarbazole) contents, up to 30 wt.%, significantly enhanced the dielectric constant, up to 9 at $10^3$ Hz, relative to the neat epoxy matrix, owing to the poly(N-vinylcarbazole) microdomain formation and strong polarization effects in the matrix (Fig. 4 B). According to Fig. 4 C, including poly(ethylene oxide)-fullerene contents, of 12 wt.%, in the epoxy matrix resulted in a higher dielectric constant, of 8.5, relative to the neat epoxy, due to the aromatic conjugation and electron polarization

effects in the epoxy/fullerene-poly(ethylene oxide) nanocomposite, whereas dielectric loss values seemed to be unaffected. Moreover, Fig. 4 D shows that including poly(ethylene oxide)-fullerene contents, of 3-12 wt.%, in the epoxy/poly(ethylene oxide)-block-poly(N-vinylcarbazole) (30 wt.%) blend declined the dielectric constant values, from 7 to 4, (dielectric loss unchanged), relative to the neat epoxy, due to the formation of charge transfer complexes in turn hindering the electron passage through the poly(N-vinylcarbazole) phases and lack of electron polarization effects in the matrix.

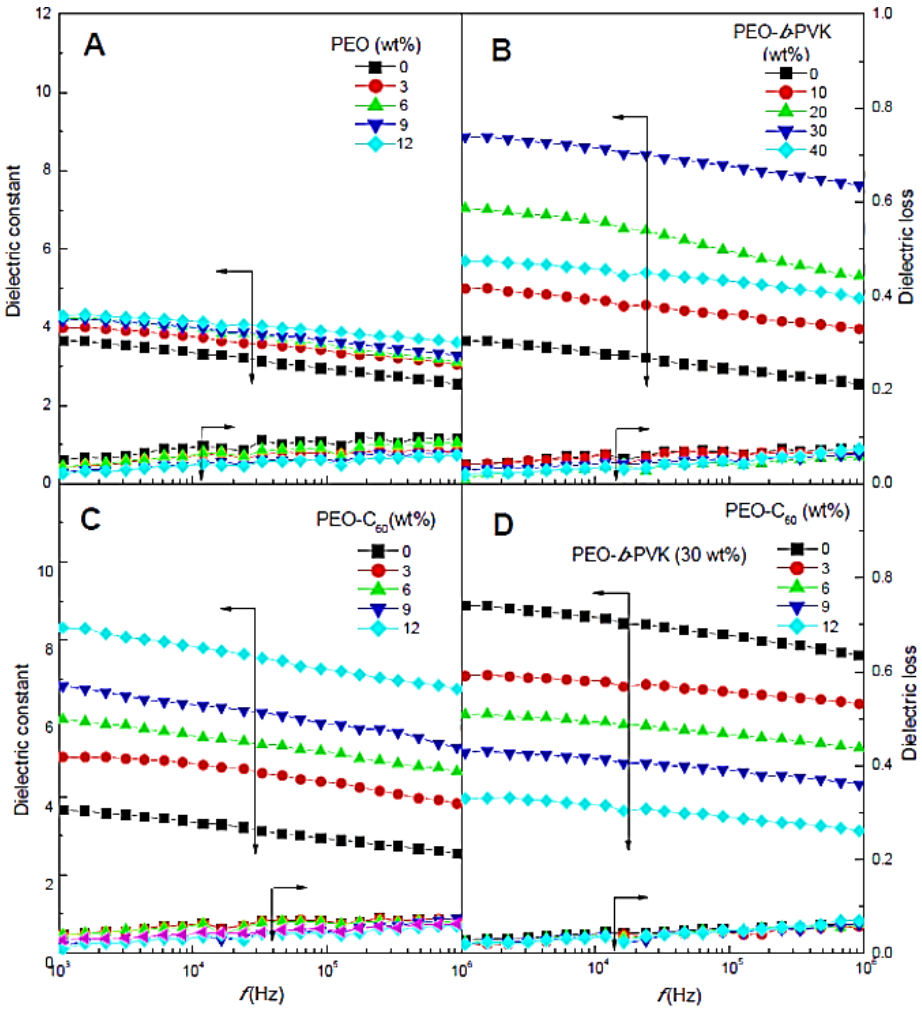


**Fig. 4.** Plots of (A & C) dielectric constant and (B & D) dielectric loss as functions of AC frequency, where: (A) the binary blends of epoxy having 3-12 wt.% of PEO; (B) the epoxy thermosets containing 3-12 wt.% of PEO-b-PVK; (C) the epoxy thermosets with 3-12 wt.% of PEO-$C_{60}$; and (D) the epoxy thermosets containing 30 wt.% of PEO-b-PVK and various amounts of PEO-$C_{60}$ (3-12 wt.%). Here PEO = poly(ethylene oxide); PEO-$C_{60}$ fullerene-poly(ethylene oxide); PEO-b-PVK = poly(ethylene oxide)-block-poly(N-vinylcarbazole). Reproduced from [43] with permission from Elsevier

Das et al. [44] formed fullerene $C_{60}$ reinforced diglycidyl ether of bisphenol A epoxy nanocomposites, by using triethylenetetramine as a hardener, through a simple ultrasonic technique and investigated their mechanical properties. For stress-strain analysis, neat epoxy, pristine fullerene filled epoxy matrix nanocomposites and surface modified fullerene filled epoxy matrix nanocomposites were analyzed. In this study, surface modification of the fullerene molecules was performed using an oxidation route, based on a mixture of nitric and sulfuric acids, for the formation of oxidized nanoparticles. According to the stress strain scans, including surface modified fullerene nanoparticles resulted in higher tensile strength and elastic modulus, by 23 and 46 %, respectively, relative to the neat epoxy, due to the

positive effect of fullerene surface oxidation in developing physical associations with the macromolecular chains (Fig. 5 A). Comparatively, including pristine fullerene nanofiller in the epoxy matrix caused a lesser rise in the tensile strength and Young's modulus, by 13 and 17%, respectively, as compared to the neat epoxy, due to lack of physical interactions between the matrix-nanofiller and meager reinforcing effects of the fullerene nano-additives in the matrix. Moreover, single edge notch bending test was performed to analyze the fracture toughness of the samples through a three point bending fixture procedure, as shown in Fig. 5 B.

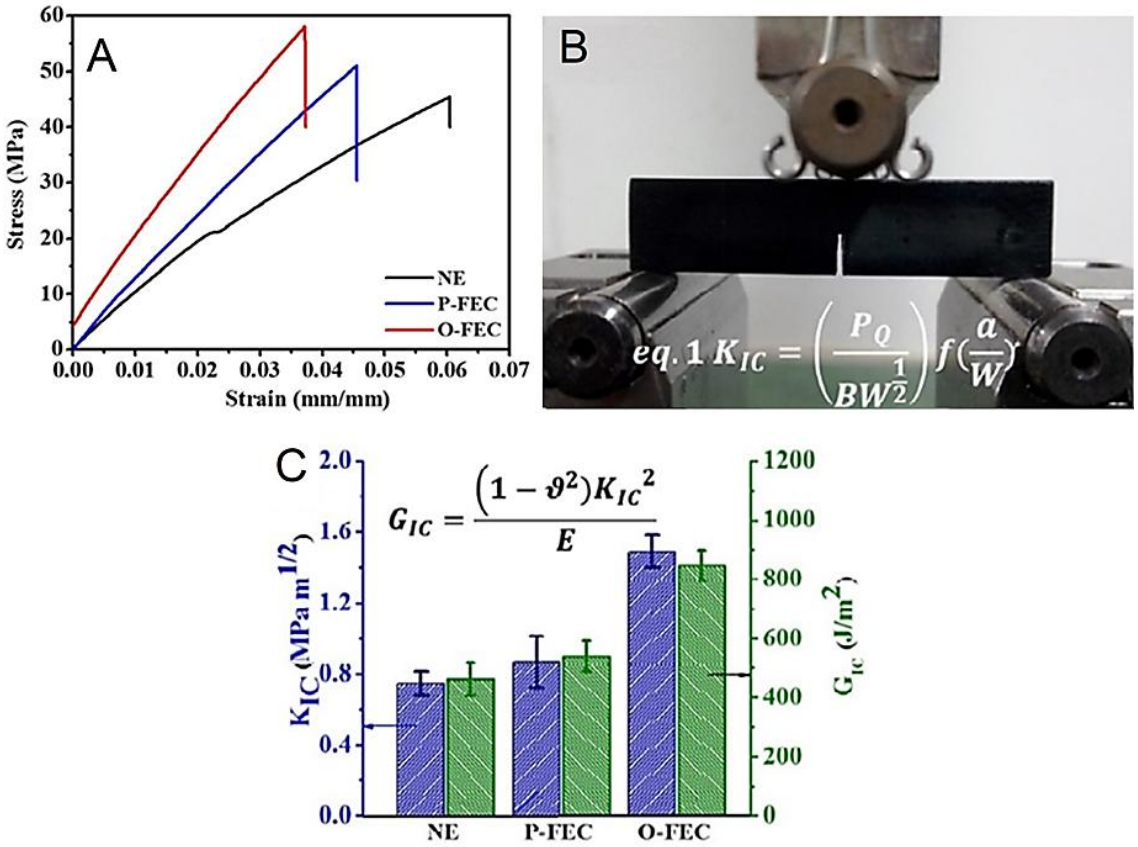


**Fig. 5.** (A) Stress-strain plot of the NE, P-FEC and S-FEC samples. (B) A diagram of SENB test procedure (performed on specimens having geometry, of 53 x 12 x 6 mm$^3$, according to ASTM D-504), inset showing an equation used for $K_{IC}$ calculation. (C) Variations of $K_{IC}$ and $G_{IC}$ for NE, P-FEC and S-FEC samples. Here NE = neat epoxy; P-FEC = pure fullerene filled epoxy matrix nanocomposite; S-FEC = surface modified fullerene filled epoxy matrix nanocomposite; SENB = single edge notch bending; $K_{IC}$ = fracture toughness; $G_{IC}$ = strain energy release rate. Reproduced from [44] with permission from Elsevier

According to the results (Fig. 5 C), including surface functional fullerene resulted in superior fracture toughness and strain energy release rate of, 101 and 85 %, correspondingly, with respect to the neat matrix, showing an obvious effect of fullerene surface modification to form non-covalent linkings with the macromolecular backbones. On the other hand, tensile strain and toughness properties of the epoxy/non-functional fullerene nanocomposites seemed to be reduced, relative to the functional fullerene based nanomaterials, probably due to the stress meditation effects of the macromolecular chains around the nanofiller nanoparticles in the matrix. As per analysis, overall enhancements in the mechanical property profiles of the epoxy/functional fullerene nanomaterials strongly depend upon the macromolecular chain interactions, i.e., hydrogen bondings, with the oxidized fullerene nanoparticles, nanofiller dispersion and compatible interface formation between the epoxy-fullerene phases.

Rafee et al. [45] fabricated the nanocomposites of diglycidyl ether of bisphenol A epoxy filled with fullerene $C_{60}$ nanoparticles, in the range of 0.1 to 1 wt.%, by simple sonication and solution routes. According to scanning electron microscopy micrographs (Figs. 6 A a & b), fullerene nanoparticles (1 wt.%) seemed to be dispersed in the aggregated macromolecular domains, due to high molecular weight of the matrix. Fig. 6 B shows the stress-strain plots of the diglycidyl ether of bisphenol A/$C_{60}$ nanocomposites with the nanofiller contents, of 0.1 to 1 wt.%. According to the results, including the 1 wt.% fullerene nanoparticles increased the Young's modulus and ultimate tensile strength, by 19 and 20 %, respectively, relative to the neat epoxy matrix.

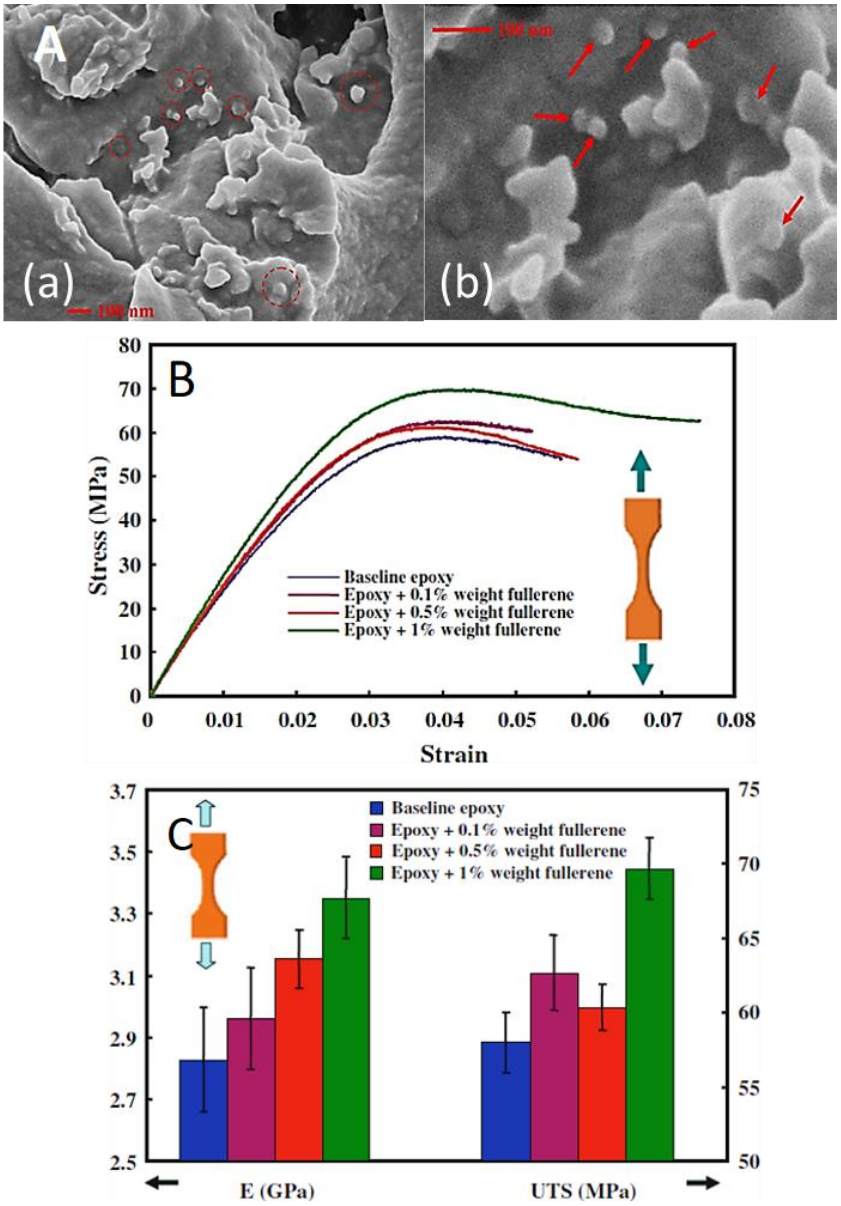


**Fig. 6.** (A) Scanning electron microscopy images of the fractured surface of the (a) nanocomposite sample indicating 1 wt.% $C_{60}$ nanoparticles, indicated by red circles, dispersed in the epoxy matrix; and (b) the micrograph of the same sample having visible polymer aggregates, whereas the $C_{60}$ nanoparticles are indicated by arrows. (B) Typical stress strain curves of the neat epoxy and the epoxy/fullerene nanocomposites, where inset shows dog bone shaped samples used in the tensile testing. (C) Plots of Young's modulus (E) and ultimate tensile strength (UTS) of the baseline epoxy and the epoxy/fullerene nanocomposites having various $C_{60}$ nanoparticles contents, of 0.1, 0.5, and 1 wt.%, dispersed in the matrix, where inset shows dog bone shaped samples used in the uniaxial tensile testing. Reproduced from [45] with permission from Springer.

For a comparative analysis of the stress-strain data from Fig. 6 B, Fig. 6 C demonstrates the bar plots of Young's modulus and ultimate tensile strength of the pristine epoxy and the epoxy/fullerene nanocomposites having various nanofiller contents, of 0.1-1 wt.%, indicating a positive influence of the nanofiller loadings on the mechanical properties of the matrix. It can be suggested that enhancements in the mechanical properties of the pristine epoxy resin with fullerene can be attributed to the formation of optimal non-covalent interactions (hydrogen bindings and π-π interactions) between the macromolecular backbones and the nano-additives, therefore leading to the development of a compatible epoxy/fullerene interface and noticeable nanoparticle reinforcement effects.

## CONDUCTIVE POLYMER/FULLERENE NANOCOMPOSITES HAVING PHYSICAL INTERACTIONS BETWEEN MACROMOLECULAR MATRICES AND NANOFILLERS

Like thermosets, conductive matrices have also been considered important to form nanocomposites with carbon nanoparticles. Unlike thermosets or thermoplastics, conducting or conjugated polymers are organic macromolecules having alternating single- and double bonds in their semiconducting backbones [46]. Owing to valuable optical properties, electron/thermal conductivity, heat stability and anticorrosion characteristics, various conductive polymers, like polyaniline, polypyrrole and polythiophene, have been fabricated and analyzed for scientific applications in the electronics/energy devices, corrosion resisting coatings and allied technological fields [47, 48]. According to the literature so far, including carbon or inorganic nanoparticles in the conjugated matrices caused noticeable enhancements in the structural, thermal stability, mechanical strength and chemical stability of the ensuing nanocomposites, compared with pristine polymers, due to the nanoparticle scattering and physical associations with the semiconducting macromolecules [49]. Consequently, the resulting conjugated matrix/carbonaceous nanoparticle nanomaterials revealed potential for myriad of applications in the fields of photovoltaics, sensors, supercapacitors, batteries, engineering structures and biomedical systems, to name a few [50].

Fullerene has been characterized as one of most valuable nano-additives among zero dimensional carbonaceous nanoparticles, like nanodiamonds, nanoonions and carbon black, for formation of conductive matrix nanocomposites [51]. Among semiconductive organic macromolecules, like polypyrrole, polythiophene and polythiophene derivatives, polyaniline owns a distinct structure consisting of six membered heterocyclic (heteroatom is nitrogen) carbon rings in its backbones [52]. Consequently, various facile methods have been reported in the literature for the preparation of polyaniline through the polymerization of aniline monomers [53]. Depending upon the synthesis method used, polyaniline generally exists in numerous oxidation states, like pernigraniline, emeraldine and leucoemeraldine; where the most commonly studied oxidation state in the literature is the emeraldine base. Essential physical characteristics, including electron/charge/heat conductivity and mechanical robustness, of polyaniline seemed to be enhanced through reinforcement with various nanofillers, like nanocarbons and metal nanoparticles [54]. As per research reports up till now, the nanocarbon nanoparticles filled polyaniline revealed superior physical properties, relative to the pristine polymer and the polyaniline/inorganic nanomaterials, and technical applications for advanced energy and electronics devices/systems [55]. In due course, Zubtsova et al. [56], reported on a complex formation between the polyaniline-fullerene due to physical interactions between the phases. The resulting nanomaterials were studied using the S-type liquid crystal cells having initial planar orientations. Herein, physical associations

of the conjugated macromolecules with the nanofiller were responsible for the generation of nematic liquid crystals in the matrix. Xiong et al. [57] applied an *in situ* polymerization technique for the formation of fullerene $C_{60}$ reinforced emeraldine base type polyaniline nanocomposites. This study analyzed the electron donor-acceptor linkings between the macromolecular chains and the nanoparticles; thus, leading to facilitated electron transportations through the physically interlinked polyaniline/fullerene nanocomposites. Recently, Mathew et.al. [58] designed polyaniline/fullerene nanocomposites and studied variations in their nonlinear optical bistability by changing fullerene concentrations. It was observed that rising fullerene contents in these nanocomposites changed saturable absorption to reverse saturable absorption, due to charge transfer complex formation in polyaniline-$C_{60}$ system. Thus, superior nonlinear optical bistability of polyaniline/fullerene nanocomposites was observed at higher fullerene contents.

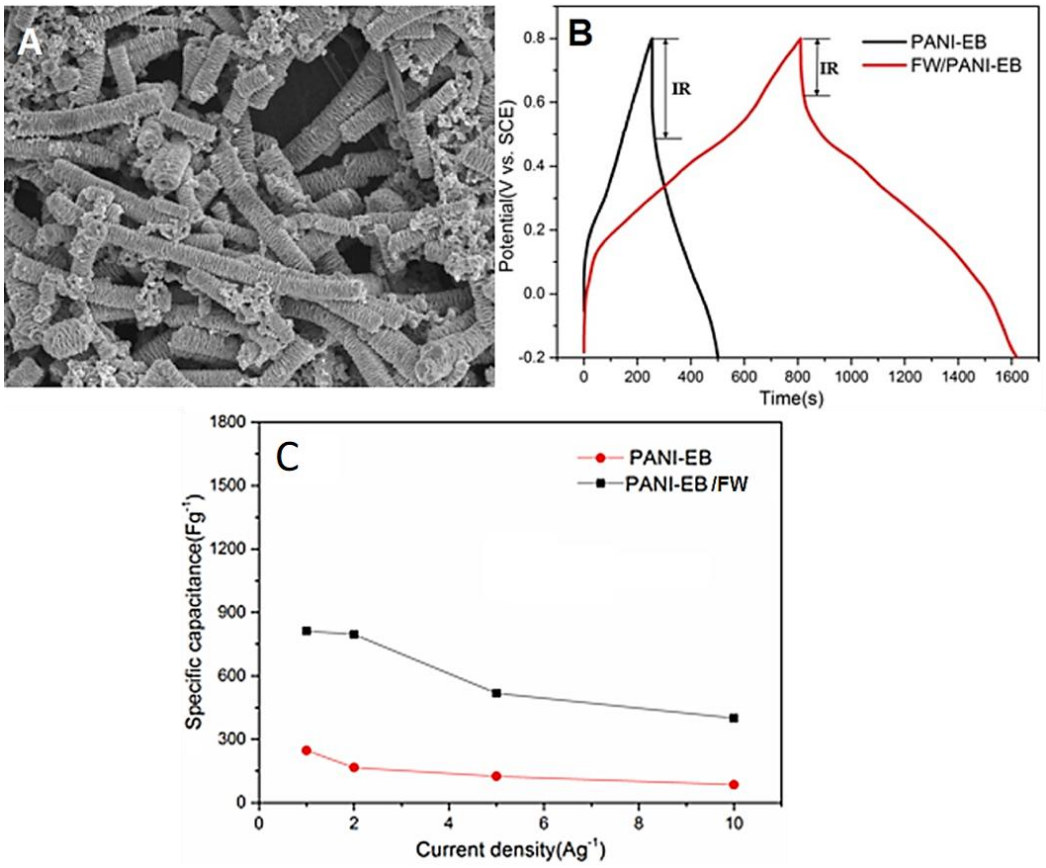


**Fig. 7.** (A) Scanning electron microscopy image of the PANI-EB/FW nanocomposite. (B) The galvanostatic charge/discharge (GCD) curves of the pristine PANI-EB and the PANI-EB/FW nanocomposite at a current density, of 1 $Ag^{-1}$, respectively. (C) The specific capacitance vs. current density plots of the pristine PANI-EB and the PANI-EB/FW nanocomposite. Here PANI-EB = polyaniline emeraldine base; PANI-EB/FW = polyaniline emeraldine base/fullerene $C_{60}$ whisker Reproduced from [59] with permission from Elsevier

Similarly, Wang et al. [59] applied in situ method to reinforced the fullerene $C_{60}$ molecules in the polyaniline emeraldine matrix. As per scanning electron microscopy analysis (Fig. 7 A), the nanocomposite revealed a unique morphological pattern having randomly oriented fullerene $C_{60}$ nanowhiskers with the polyaniline emeraldine base deposited on their surfaces, probably due to the optimal electrostatic interactions between the macromolecular chains and fullerene nanoadditives. According to galvanostatic charge-discharge analysis (Fig. 7 B), the polyaniline/fullerene nanowhiskers nanocomposite had a more symmetrical triangular curve, than the polyaniline emeraldine base, depicting an

optimum capacity and reversible electrochemical cyclic behavior of the conjugated matrix nanocomposite. Consequently, the polyaniline emeraldine base/fullerene $C_{60}$ nanowhiskers nanomaterial had a higher specific capacitance, of 813 $Fg^{-1}$, than the neat polymer (248 $Fg^{-1}$), as shown in Fig. 7 C. The nanocomposite revealed capacitance retention of > 85 % (1500 cycles). It can be suggested that electrostatic interactions between the macromolecular matrix-fullerene were accountable for a facilitated charge/electron flow through the matrix; therefore, significantly enhancing the specific capacitance of the polyaniline/fullerene nanocomposite, relative to pristine polyaniline, which can be valuable for their future application in supercapacitor electrodes. In recent times, Riaz et. al. [60] designed polyaniline, fullerene, and halide perovskite ($CsInCl_3$) based hybrids through sol gel autocombustion approach. The resulting polyaniline/fullerene/$CsInCl_3$ nanocomposites revealed notably superior specific capacitance and power density of 1800 $Fg^{-1}$ and 1400 W $Kg^{-1}$, respectively. Thus, polyaniline/fullerene/$CsInCl_3$ nanocomposites were applied as high performance electrodes for advanced supercapacitors.

Polypyrrole is also a technically valuable conductive polymer which is made up of five membered heterocyclic (heteroatom is nitrogen) carbon rings in its main chains [61]. Owing to semiconducting backbone structure, polypyrrole has fine electron conductivity characteristics, however the presence of heterocyclic conjugated monomeric units in its backbone decresaed its processability and solubility properties in organic solvents [62]. Consequently, to improve the solubility properties and related physical property-performance of polypyrrole, doping practices using various chemicals/materials, like acids, bases, metal nanoparticles and carbon nanoparticles, have been widely investigated for polypyrrole modification in the literature [63]. Consequently, literature reports regarding easily processible high performance polypyrrole/fullerene nanocomposite systems have been noticed [64]. Zhou et al. [65], for instance, explored the effect of fullerene nano-reinforcements on the structure, solubility/physical properties, and photovoltaic application of polypyrrole based nanomaterials. Moreover, Wysocka-Zolopa et al. [66] reported on the fabrication of non-covalently associated polypyrrole-fullerene $C_{60}$ nanocomposites via an in situ oxidation method. As per the microscopic studies (Fig. 8 A), fullerene nano-additives having sizes, of ~ 200-500 nm, seemed to be randomly dispersed in the polypyrrole matrix. Additionally, the polypyrrole/$C_{60}$ nanocomposites were studied for their density of states and band structure properties, as shown in Fig. 8 B. According to density of states plots of the nanocomposites (left image in Fig. 8 B), variation in the band structure from lowest to highest occupied molecular orbital (right image in Fig. 8 B) resulted in a band gap, of 0.25 eV, owing to physical interactions between the polypyrrole-$C_{60}$ responsible for rapid electron transfer at their interfaces [67]. Nevertheless, very limited literature repots up till now were noted regarding non-covalently associated fullerene doped polypyrrole based nanocomposite systems, therefore focused future research endeavors seemed to be indispensable to reveal the structure, physical attributes and technical potential of these innovative nanomaterials.

Polythiophene, having five membered heterocyclic (heteroatom is sulfur) carbon rings in its backbones, is another worth mentioning heterocyclic macromolecule from the family of semiconducting polymers [68]. In addition to facilitated electron transference properties, polythiophene has been studied for its optical, electrochemical, thermal and environmental stability characteristics [69]. In this regard, various easily soluble and processable derivatives of polythiophene have been reported in the literature, like poly(3-hexylthiophene), poly(3-dodecylthiophene), poly(3-octadecylthiophene) and so on [70]. Additionally, doping of polythiophene with nanocarbon nanoparticles has been observed to enhance the electrical

conductivity and applied potential of the ensuing nanocomposites, compared with the pristine polythiophene, for the solar cells, batteries, capacitors and allied electronics/energy devices [71]. Subsequently, poly(3-hexylthiophene), an important polythiophene derivative, has been observed to form high performance nanocomposites with various carbon nanoparticles, like nanodiamonds, graphene and allied nanocarbons [72]. Successively, a few literature reports were observed on the advanced fullerene reinforced poly(3-hexylthiophene) nanocomposites [73]. In these poly(3-hexylthiophene)/fullerene nanomaterials, fullerene generally acts as an electron donor, whereas the conjugated polymer behaves as an electron acceptor. In this way, electron donor-acceptor associations and electrostatic interactions have been observed in the fullerene reinforced poly(3-hexylthiophene) nanocomposites to facilitate the electron passage through their backbones.

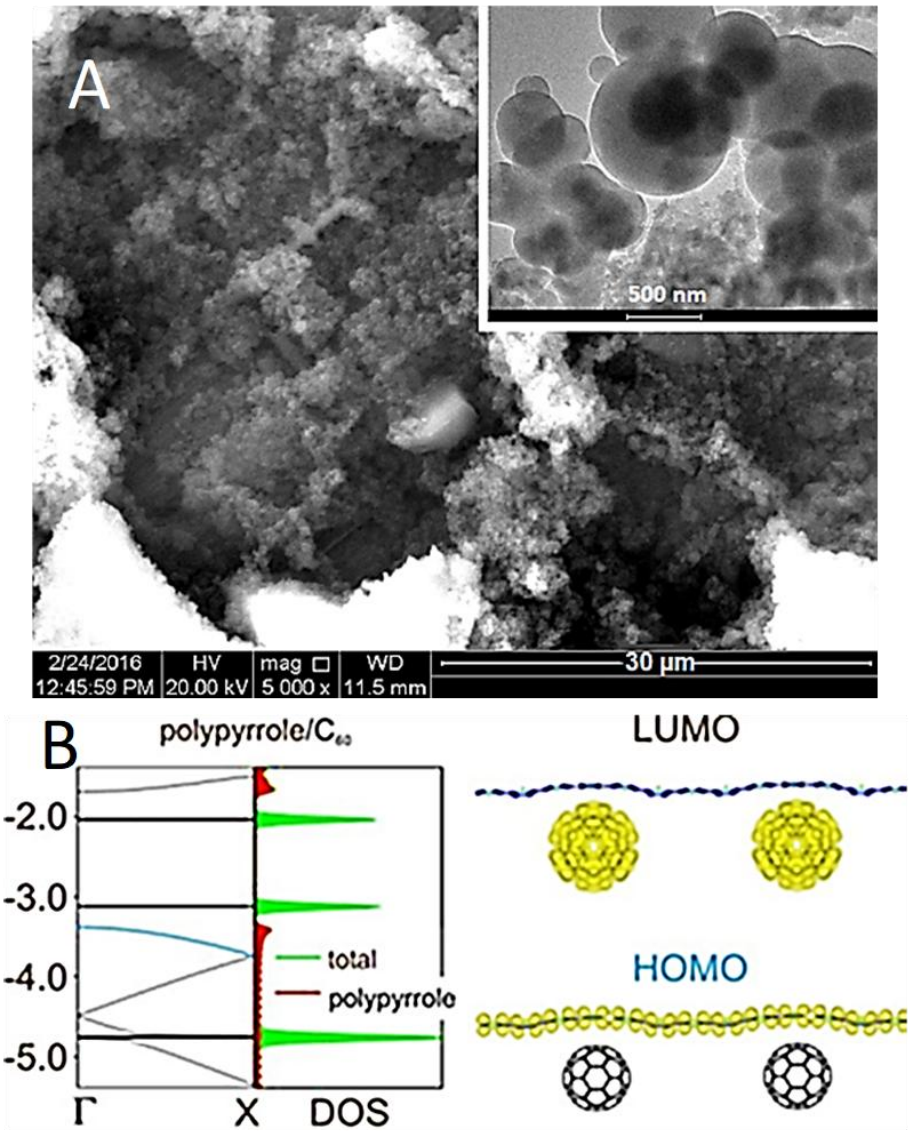


**Fig. 8.** (A) Scanning electron microscopy image with an inset of transmission electron microscopy image of the polypyrrole/$C_{60}$ nanocomposite. (B) The density of states (DOX) plots (left) and the band structure (right) of the polypyrrole/$C_{60}$ nanocomposite. Reproduced from [66] with permission from ACS

Li et al. [74] examined the non-covalent interactions between the poly(3-hexylthiophene) matrix and the amine modified fullerene nanoparticles based hybrids processed through a

solution route. As shown in Fig. 9 A, the carbonyl and amine functionalities of the conducting macromolecular matrix efficiently established hydrogen bonding interactions with the amine functionalities of the modified fullerene molecules. Figs. 9 B a & b show atomic force microscopy analysis of the nanocomposites of poly(3-hexylthiophene) and modified fullerene molecules mixed in different ratios, of 10:8 and 10:10, respectively. It was observed that poly(3-hexylthiophene)/amine modified fullerene nanocomposite with matrix:nanofiller ratio, of 10:10 (Fig. 9 B a), showed a uniform nanoparticle dispersion pattern with dispersed fullerene nanoparticles, of ~ 20 nm, so validating the morphological influence of three point hydrogen bonding between the poly(3-hexylthiophene) and the modified fullerene molecules. On the other hand, the poly(3-hexylthiophene)/amine modified fullerene nanocomposite having a matrix:nanofiller ratio, of 10:8 (Fig. 9 B b), depicted larger macromolecular domains, of > 100 nm, relative to the 10:10 matrix:nanofiller sample, due to lower nanofiller contents and so the reduced interactions between the poly(3-hexylthiophene)-fullerene.

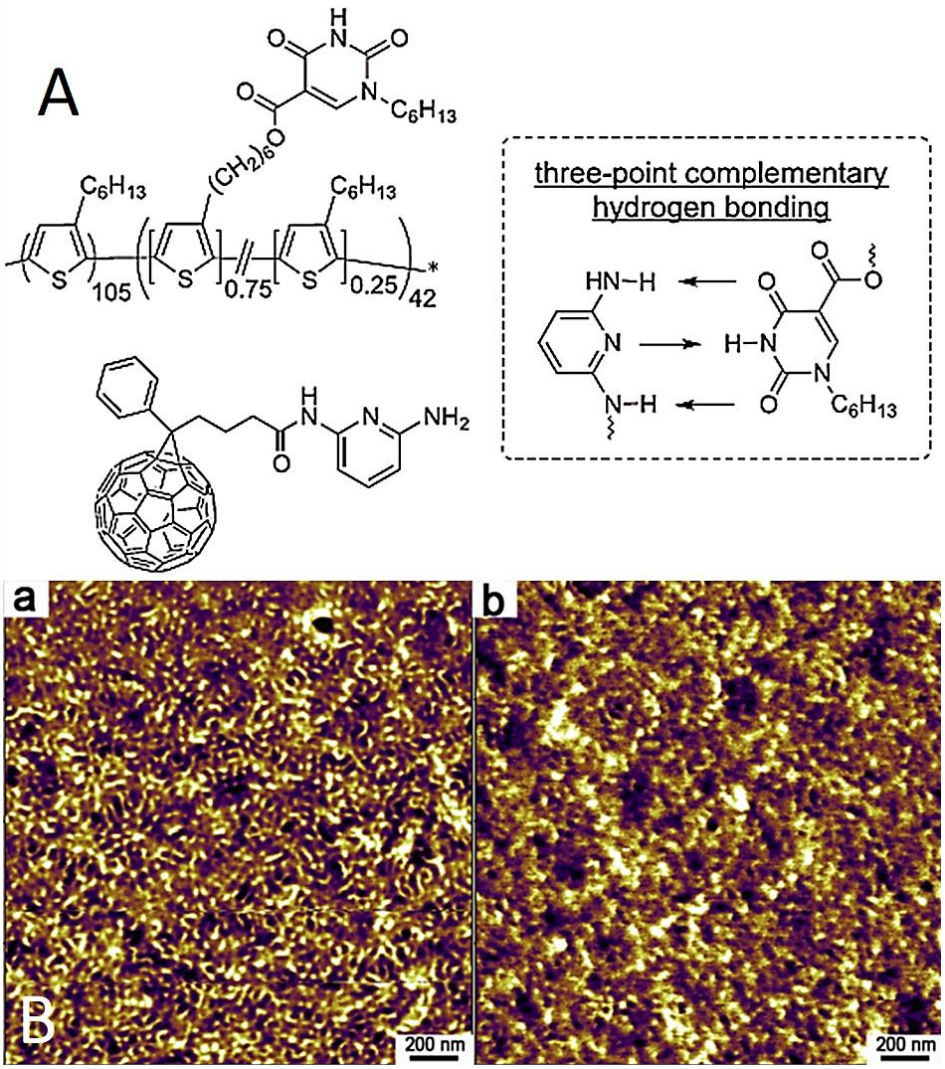


**Fig. 9.** (A) The structures (left) and hydrogen bonding interactions (right) of the conjugated block copolymer and the modified fullerene. (B) Atomic force microscopy images of the nanocomposite with block copolymer:fullerene ratio of (a) 10:10; and (b) 10:8. Reproduced from [74] with permission from Elsevier

## TECHNICAL APPLICATIONS OF PHYSICALLY INTERLINKED NANOCOMPOSITES OF THERMOSETTING OR CONDUCTIVE POLYMERIC MATRICES AND FULLERENE NANO-ADDITIVES

As per literature analysis of preceding review sections, limited research attempts have been reported in the literature up till now showing the technical worth of non-covalently associated thermosetting matrix/fullerene and conductive polymer/fullerene nanocomposites for anticorrosion coatings, solar cells and solar rechargeable battery applications.

Particularly, recent reports have been noticed regarding polythiophene/fullerene for optoelectronics [75]. In this concern, Räder et. al. [76] studied charge transfer dynamics in organic solar cells based on quaterthiophene/fullerene nanocomposites. Consequently, three distinct excitation regimes were observed, including strong field with transient effects, medium pulse intensities of 3-36GW, and Femtosecond radiations with weak pulse intensities < 3 GW. Hence, quaterthiophene/fullerene nanocomposites were applicable as high tech charge transfer donor/acceptor system in organic solar cell interfaces. Rasheed et. al. [77] designed polythiophene/fullerene nanocomposites as ionic liquid gel electrolyte for dye sensitized solar cell. The polythiophene/fullerene nanocomposite depicted electrical conductivity and ionic conductivity of > 83 S $cm^{-1}$ and ~2.0 × $10^{-2}$ mS $cm^{-1}$, respectively. The dye sensitized solar cell with polythiophene/fullerene nanocomposite based electrolyte showed power conversion efficiency ~ 8 %. Mahmoud et. al. [78] developed spin coated poly(3-hexylthiophene-2,5-diyl), [6,6]-phenyl-C61-butyric acid methyl ester, and fullerene based organic solar cells containing aluminum cathode. Herein, solar cell efficiency was affected by varying the active layer thickness. Consequently, by increasing the fullerene based nanocomposite layer thickness up to 80 nm enhanced the power conversion efficiency to > 2 %, i.e. ~ 6 % higher than the thin layered organic solar cell. It can be suggested that optimum matrix:nanofiller ratios, i.e., amounts of macromolecules and nanofillers in the nanocomposite, revealed a significant effect on the development of secondary interactions and interfacial mechanisms between the polythiophene derivative-fullerene phases. Henceforth, according to the available literature repots so far, various physical linkages, such as electrostatic, hydrogen bonding and aromatic stacking interactions, have been observed between the polythiophene derivative macromolecules and fullerene nano-additives; therefore, leading to the formation of efficient charge transfer polymer-nanofiller complexes for potential utilization as active photovoltaic layers for solar cell applications [79, 80].

### *Anticorrosion coatings*

In the case of corrosion protective coatings, generally, applied to prevent the corrosion of metal surfaces, various materials, like polymers, ceramics and organic/inorganic hybrids have been investigated in the literature [81]. Consequently, among these coating materials, polymeric macromolecules reinforced with nanocarbons/metal nanoparticles/metal oxides revealed important technological applications for corrosion protection of metals [82]. Specifically, carbonaceous nano-additives, like graphene, fullerene, nanodiamond, etc., filled polymeric nanocomposites depicted advantages of low cost, low density and facile processability to be applied as high performance corrosion prevention materials [83]. In this context, anticorrosion performance of nanocomposite coatings seemed to be strongly dependent upon the uniform nanoparticle scattering in the macromolecular matrices (having optimal molecular weights); therefore, hindering the diffusion paths of the corrosion causing percolating corrosion species, like metal ions, metal oxides, acidic species and moisture, towards the metal surfaces [84]. Subsequently, a few literature research reports so far have

been observed for the polymer/fullerene nanocomposites having non-covalent interactions, like electrostatic, hydrogen bonding, etc.) between the matrix-nanofiller; thus, enhancing the electron/charge conductivity of these nanomaterials desirable for their anticorrosion properties [85, 86]. Liu et al. [87], for instance, prepared the nanocomposites of bisphenol-A epoxy and fullerene using diethylenetrimine as a curing agent. Herein, prior to the nanocomposite formation, fullerene nanoparticles were functionalized through refluxing technique in ethanol solvent. Afterwards, the resulting functional fullerene nanoparticles, up to 0.75 wt.%, were reinforced in the bisphenol-A/diethylenetrimine system using a simple solution route and the as prepared epoxy/functional nanocomposites were investigated for their tribological and corrosion resistance features. As per microscopic examinations via transmission electron and high resolution transmission electron microscopy techniques (Figs. 10 A & B, respectively), the pristine fullerene nanoparticles had discretely dispersed spherical nanostructures.

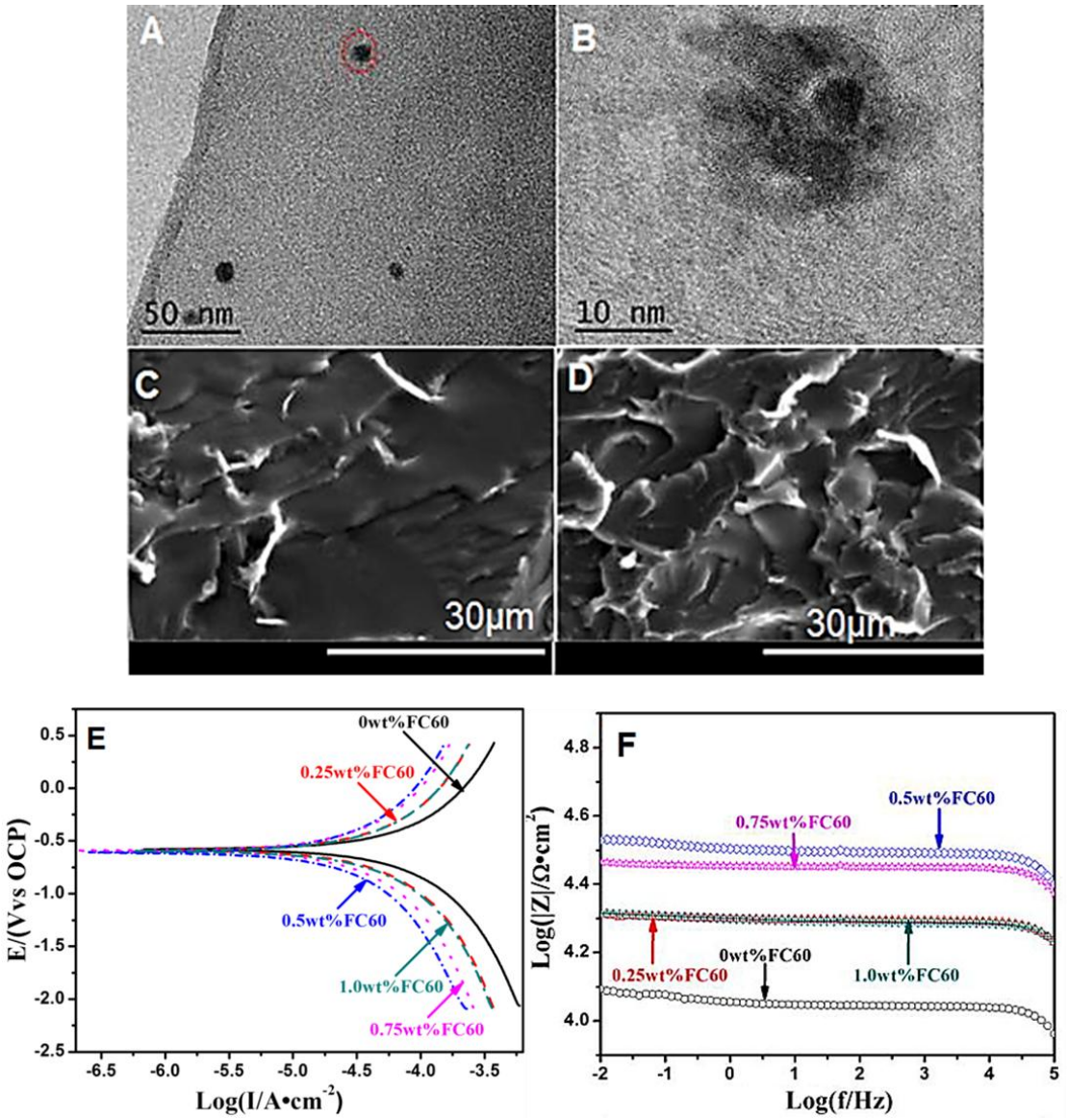


**Fig. 10.** (A) Transmission electron microscopy image of the pristine $C_{60}$ with a red encircled fullerene nanoparticle. (B) A high resolution transmission electron microscopy image of the same pristine $C_{60}$; The fracture topographies of the (C) epoxy matrix having functional fullerene contents, of 0.25 wt. %; and (D) epoxy matrix with functional fullerene contents, of 0.5 wt. %. (E) Tafel polarization curves of the epoxy/fullerene nanocomposite coatings. (F) Bode plots of the epoxy/fullerene nanocomposite coatings. Here $FC_{60}$ = ethanol treated functional fullerene. Reproduced from [87] with permission from Elsevier

On the other hand, including functional fullerene contents, of 0.25 wt.% (Fig. 10 C), in the epoxy matrix revealed a characteristic aggregated macromolecular morphology with completely merged fullerene nanoparticles and a rough fractured surface. Moreover, including higher functional fullerene contents, of 0.5 wt. % (Fig. 10 D), in the matrix visibly enhanced the macromolecular chain aggregation and roughness of the fractured surface. Here, aggregated polymer/fullerene microstructures seemed to be due to dominating effects of the macromolecular chains and lower nanofiller contents in the matrix, so leading to poor matrix-nanoparticle interactions at the matrix-nanofiller interfacial level. Additionally, corrosion resistance studies for the pristine epoxy and the epoxy/fullerene nanocomposite coatings having nanofiller contents, of 0.25-1 wt.%, were performed through Tafel polarization technique (Fig. 10 E). According to the results, a characteristic Tafel Zone was observed for the pristine epoxy and the nanocomposite coatings depicting their anticorrosion potential after being tested on the metal surface. Moreover, including fullerene contents, of 0.25-1 wt.%, enhanced the characteristic Tafel Zone of the polymer/fullerene nanocomposites, due to high aspect ratio of the fullerene nanoparticles responsible for upgrading the interfacial macromolecular-nanofiller effects and corrosion resisting potential of these coatings. In addition, the corrosion current values of the polymer/fullerene nanocomposite coatings were found lower, than the neat epoxy system, showing superior barrier characteristics of the fullerene reinforced macromolecular coatings. To further explore the corrosion resistance performance of the epoxy/fullerene coatings in 3.5 wt.% NaCl based corrosive media, Bode plots were studied, as shown in Fig. 10 F. According to the results, including fullerene contents, of 0.25-1 wt.%, upsurged the impendence modulus of the resulting epoxy/fullerene nanocomposites, relative to the neat matrix, so indicating the decline in the corrosion rate due to the effectiveness of the nanocarbon nanoparticles for creating a strong barrier towards the corrosion causing species.

Few very recent research attempts have been noticed for epoxy/fullerene hybrids for anticorrosion or antiweathering applications for resisting light, chemicals, and other environmental effects [88]. For instance, Huang et. al. [4] designed a solution casted thermoset system with polycarbonate/acrylonitrile-styrene-acrylic and modified fullerene, reduced graphene oxide, and carbon nanotube. The hybrid nanocomposite system revealed notably superior corrosion resistance and UV resistance features. Moreover, in very recent times, Babahan et. al. [89] designed bisphenol A epoxy coatings with fullerene/nanocarbons hybrid nanoadditives by employing bio based hardener (turpentine oil/moss oil). The resulting epoxy/hybrid fullerene nanoparticles nanocomposites were used as weathering resistant coatings for wood surfaces. As per total color change tests, using modified nanoparticles enhanced the resistance of epoxy coatings towards any color changes and weathering effects

*Solar cell devices*

Above and beyond anticorrosion coatings, an important technical application of the epoxy/fullerene nanocomposites has been observed for solar cell devices [90]. In this concern, most of the literature available so far reported on the covalently associated epoxy/fullerene systems for efficient solar cell utilization due to the effectiveness of the covalently interlinked macromolecular-nanofiller interfaces in enhancing the photovoltaic features; nevertheless, a limited research efforts have been noticed up till now for the non-covalently interlinked epoxy/fullerene systems for this application [91]. A few literature review articles have been noticed so far stating the application of the physically bonded polymer/fullerene systems for organic solar cell designs [92]. According to the analysis, including fullerene in polymeric matrices via physical means may reveal lower power conversion efficiencies, of 12 %,

relative to the allied covalently bonded nanocomposites having significantly higher power conversion efficiencies, of up to 20 % [93]. Han et al. [94], for example researched on the physically interacted epoxy and $C_{60}$-isobenzofulvene nanoparticles based nanocomposites, prepared via an in situ process, for photovoltaics. Consequently, the resulting epoxy/$C_{60}$-isobenzofulvene nanocomposites revealed a higher power conversion efficiency, of 3.1 %, than a comparable system of phenyl-C61-butyric acid methyl ester/$C_{60}$ (2.5 %), due to π-π interactions between the macromolecular backbone and isobenzofulvene modified fullerene nano-additives. In addition to the epoxy/fullerene nanomaterials, effects of non-covalent fullerene reinforcements on the photovoltaic characteristics of the conductive matrices have been investigated in the literature [95]. Accordingly, in conducting polymer/fullerene nanocomposites, the conjugated macromolecules seemed to have intrinsic electron/charge/hole transportation features to act as efficient electron donors, whereas fullerene molecules usually behave as electron acceptors leading to the formation of electron transfer complexes to enhance their electronic, electrochemical and nanostructural properties for photovoltaic application [96]. In this context, a few literature reports were observed regarding polythiophene derivatives and fullerene $C_{60}$ based nanocomposites for organic photovoltaic devices [97]. Lobez et al. [98], for instance, developed a photovoltaic system based on the physically interlinked poly(3-hexylthiophene)/phenyl-C61-butyric acid methyl ester and fullerene nanoparticles. Fig. 11 A shows a snapshot of the proposed nanoscale organizations within the binary poly(3-hexylthiophene)/phenyl-C61-butyric acid methyl blend and the fullerene nanoparticles. Consequently, the nanoparticles formed ordered orientation between the macromolecular chains leading to the crystallinity properties of the matrix-nanofiller system. Fig. 11 B a shows a photograph of dipole formation in the poly(3-hexylthiophene)/phenyl-C61-butyric acid methyl ester/fullerene nanocomposite, which seemed to be due to the development of the macromolecular (poly(3-hexylthiophene)/phenyl-C61-butyric acid methyl ester)-fullerene heterointerfaces having low charge carrier recombinations. Moreover, including fullerene nano-additives, of 0.25 wt.%, resulted in a higher photo conversion efficiency, of about 30 % (Fig. 11 B b), relative to the neat blend matrix, due to the development of effective dipole interactions and interfaces between the conjugated macromolecules and the fullerene nanoparticles responsible for their superior photovoltaic performance.

*Batteries*

Additionally, conjugated polymers, like polyaniline, having p-type semiconductivity and photosensitivity properties were investigated for the solar chargeable batteries [99]. Especially, the polyaniline/$C_{60}$ systems have been observed competent for developing active hole-electron pairs to electrochemically transform the solar energy into the chemical energy for the desirable battery application [100]. Tran et al. [101], for example, studied the electron transference properties of the polyaniline/fullerene plasma-induced carbon clusters nanocomposites. Relative to the neat polyaniline matrix, the resulting nanocomposite had higher capacity, of 310 mAh $g^{-1}$, capacity retention, of 91 % (2000 cycles) and photon energy conversion efficiency, of 1.15 %, due to the efficiency of fullerene plasma-induced carbon clusters for developing photoexcited electrons/holes in the matrix. Fig. 12 a shows a snapshot of the fiber shaped solar rechargeable battery design consisting of a polyaniline/fullerene plasma-induced carbon clusters based photocathode and a polyaniline/fullerene plasma-induced carbon clusters/zinc hybrid based photoanode. Scanning electron microscopy images of the polyaniline/fullerene plasma-induced carbon clusters hybrid (Figs. 12 b & c) revealed a typical aggregated conjugated macromolecular morphology along with a few distinctly dispersed polyaniline nanofibrils having diameter, of 100 nm. Moreover, an energy band

diagram (Fig. 12 d) of the polyaniline and the fullerene plasma-induced carbon clusters was studied to analyze the exact positions of their valence and conduction bands before their mutual interactions/contact in the battery.

Henceforth, potential of non-covalently interacted polyaniline-fullerene nanocomposites for efficient solar rechargeable battery electrodes was analyzed, nevertheless only limited literature has been published up till now, for these next generation conductive polymer/fullerene based technological materials.

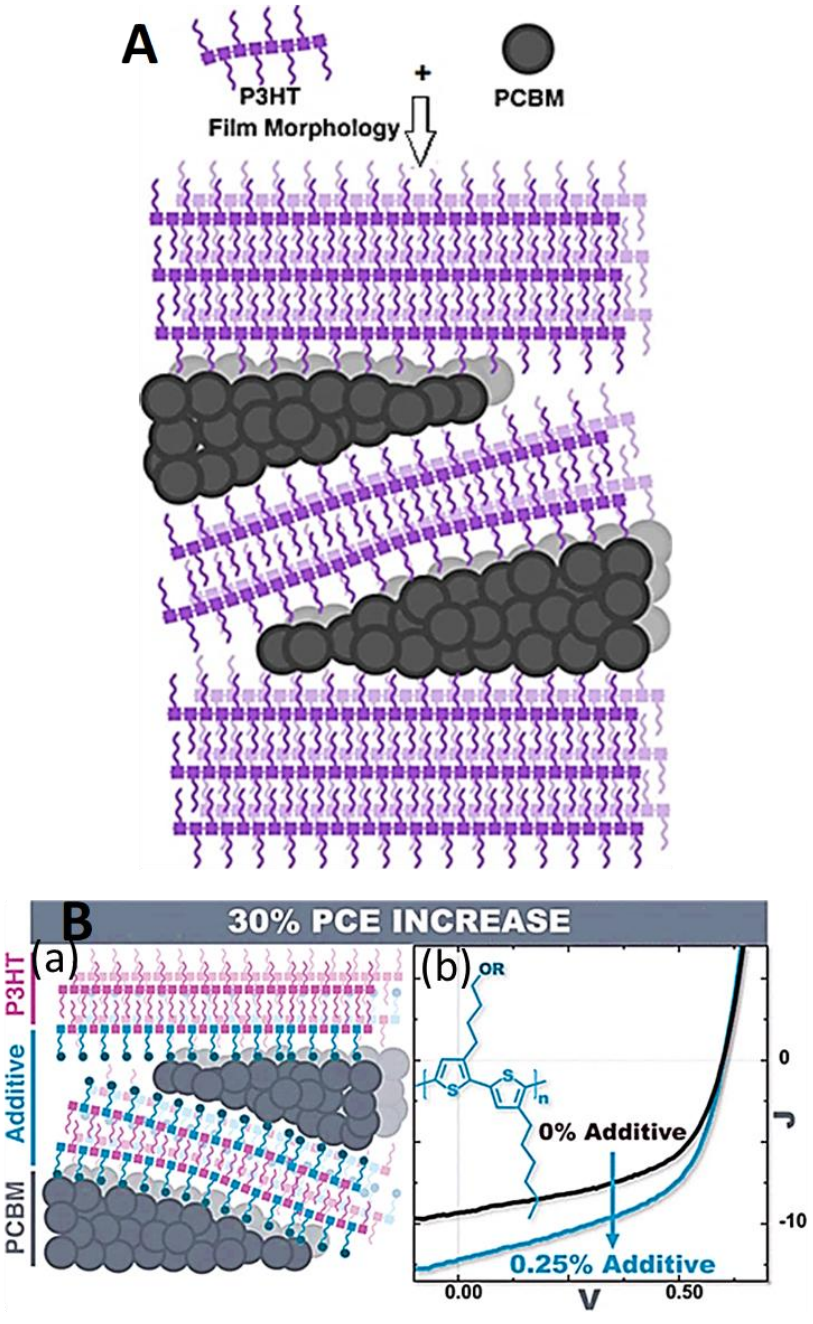


**Fig. 11.** (A) Diagram of the proposed nanoscale organizations within a binary mixture of P3HT and PCBM matrices; (B) (a) A snapshot of the dipole formation due to the development of the polymers (P3HT and PCBM)-fullerene heterointerfaces. (b) Current-voltage plots showing a 30 % enhancement in the PCE of the P3HT:PCBM based solar cell with the fullerene contents, of 0.25 wt.%, relative to the neat P3HT:PCBM matrix. Here PCBM = Phenyl-C61-butyric acid methyl ester; P3HT = poly(3-hexylthiophene); PCE = photo conversion efficiency. Reproduced from [98] with permission from ACS

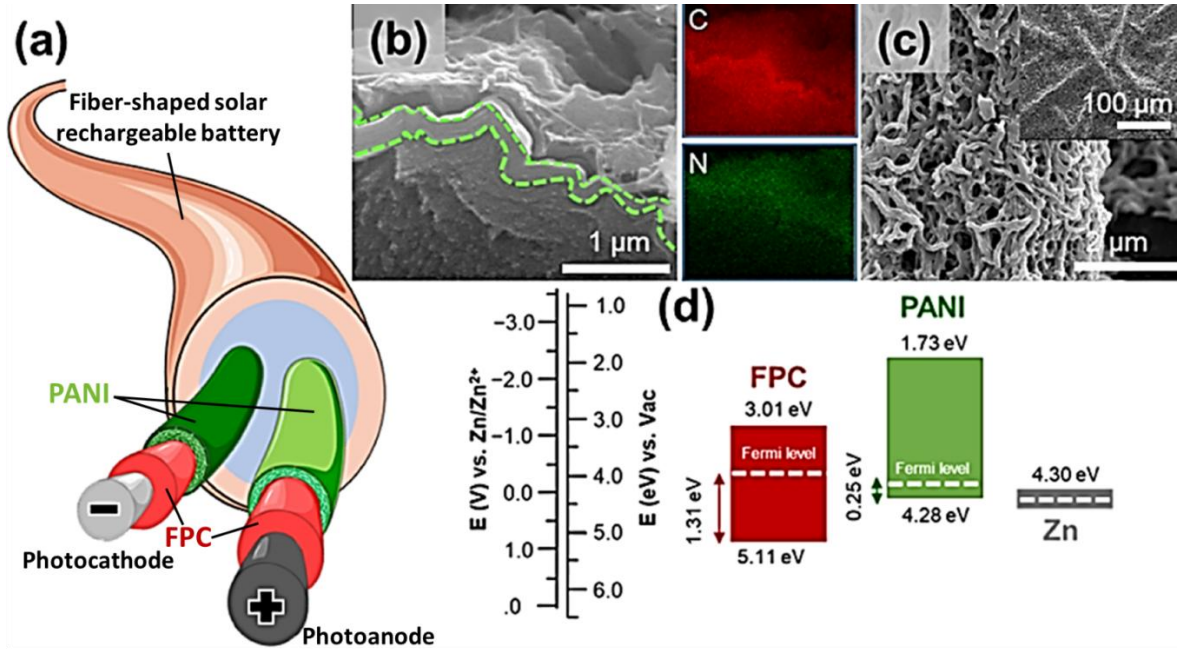


***Fig. 12.*** *Characteristics of the polyaniline-fullerene plasma induced carbon clusters (PANI-FPC) heterojunction in the flexible solar rechargeable battery: (a) a schematic of the fiber-shaped solar rechargeable battery consisting of a PANI-FPC based photocathode and a PANI-FPC@Zn based photoanode. Scanning electron microscopy images of: (b) a cross-section (left) of the PANI-FPC sample, where green dotted lines show polyaniline nanofiber having diameter, of 100 nm, and the corresponding energy dispersive X-ray spectrometry mapping (right); and (c) top-view of the PANI-FPC surface. (d) An energy band diagram for the PANI and the FPC before mutual interactions/contact. Here FPC = fullerene plasma-induced carbon clusters; PANI = polyaniline. Reproduced from [101] with permission from Elsevier*

## VIEWPOINTS, FUTURE OPPORTUNITIES AND CONCLUSIONS

Above presented to date research progress in the field of non-covalently associated thermosetting matrix/fullerene and conjugated polymer/fullerene hybrids revealed significant scientific potential for corrosion protection coatings, solar cells and solar rechargeable battery applications (Fig. 13 & Table 2) [102-104].

As per literature analysis, including modified fullerene nanoparticles in the thermosetting polymers have been observed advantageous for developing non-covalent interactions with the macromolecular backbones, uniform nanofiller dispersions and superior electron/charge transfer properties desirable for high-tech corrosion resistance and photovoltaic applications [105]. On the other hand, the conductive macromolecular systems non-covalently reinforced with the fullerene nanoparticles have been investigated for solar cells and solar rechargeable battery devices, whereas the available literature to date is still lacking the research reports on the physically associated conjugated polymer/fullerene nanomaterials regarding their application for anticorrosion coatings [106]. Herein, it is suggested that development of electron donor (conductive macromolecule)-acceptor (fullerene) complexes seemed to be indispensable for facilitated electron/charge transportation through the non-covalently interlinked nanocomposites for their effective utilization in solar cell devices [107]. Owing to the growing scientific concerns regarding the development of non-covalently associated thermosetting matrix/fullerene and conjugated polymer/fullerene nanocomposites for solar cells and batteries, focused research investigations may unveil significant future applications of these technically valuable fullerene based nanocomposites for supercapacitors and allied

high end energy devices [108-110]. Furthermore, among nanocarbons, using zero dimensional fullerene nanoreinforcements with thermosetting and conjugated matrices has also been found advantageous, relative to several reported allied hybrid systems with two dimensional graphene and one dimensional carbon nanotube additives (Table 3).

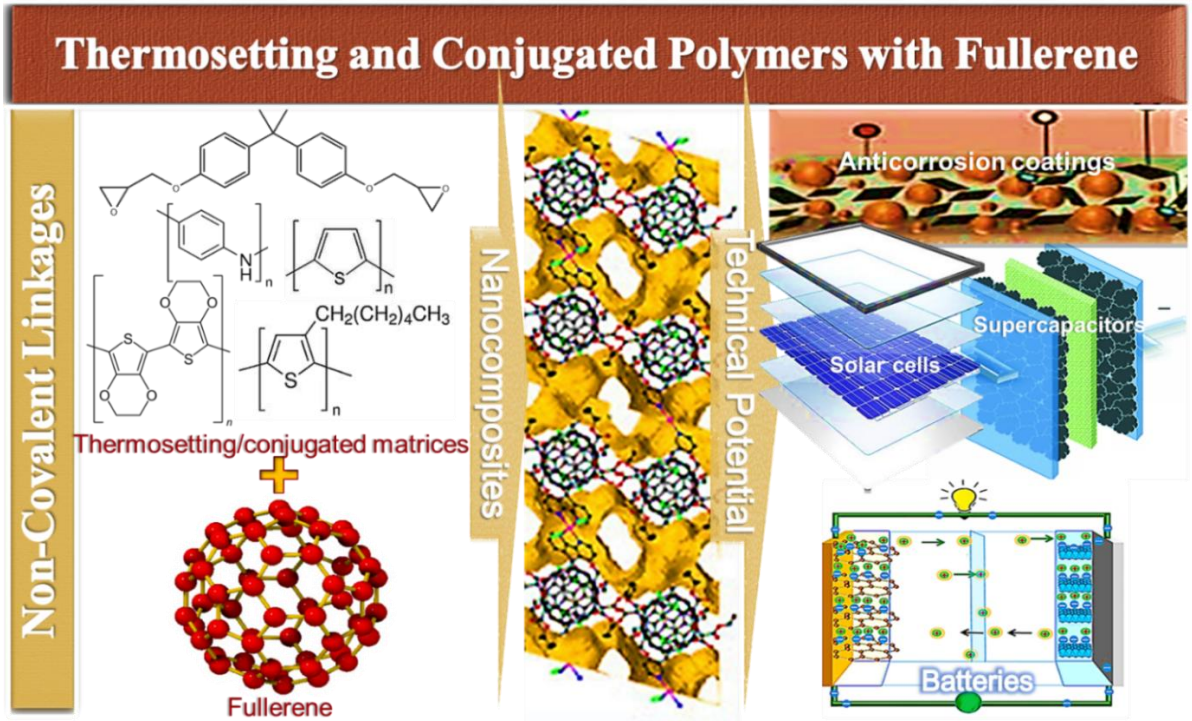


**Fig. 13.** A snapshopt of, design—to—applications, thermosetting and conjugated matrix nanocomposites with fullerene nanoadditives

Non-covalent interactions between epoxy/fullerene and conductive polymer/fullerene rely upon *(i)* processing technique, *(ii)* processing conditions/parameters, and *(iii)* surface functionalities of fullerene nanoparticles. Facile processing techniques for polymeric nanocomposites usually determine long-term stability of nanoparticle dispersions in soluble matrix phases [111]. Processing technique as well as conditions may notably contribute to nanoparticle dispersion and the final nanocomposite properties. In other words, using two different synthesis routes may result in different polymer chain conformations near nanoparticle surface despite the same matrix-nanofiller composition. Accordingly, flow and integrity of polymer chains greatly rely on synthesis technique as well as parameters adopted. For example, using sonication/stirring type techniques in assistance with solution processing or curing method may cause better flow of polymer chains to dispersed fullerene nanoparticle surfaces. This effect not only enhance matrix-nanofiller interlinking but also improve microstructural features via interfacial associations. Physical interactions between epoxy or conjugated matrices and fullerene molecules usually improve by nanoparticle dispersion in matrices. For better dispersed nanoparticles, polymer chains can easily flow towards high surface area nanoparticles; thereby increasing the physical interlinks between them. In situ technique involves the formation of polymer chains in the presence of dispersed nanoparticles. Usage of supplementary approaches (ultrasonic, magnetic stirring) along with in situ techniques usually help in uniform nanoparticle dispersion and assist physical interactions with growing polymer chains and hinder polymer chain rupture.

***Table 2.*** *Design, fabrication strategies and physical characteristics of the non-covalently interacted thermosetting polymer/fullerene and the conjugated polymer/fullerene nanocomposites*

| Matrix | Nano-additive | Fabrication | Features | Ref. |
|---|---|---|---|---|
| Epoxy/poly(ethylene oxide); epoxy/poly(ethylene oxide)-block-poly(N-vinylcarbazole) | Fullerene-poly(ethylene oxide); fullerene-poly(N-vinylcarbazole) | Click reactions; solution method; curing technique | Charge transfer complexes; nanodomain morphology; aromatic conjugation; electron polarization; dielectric constant | [43] |
| Diglycidyl ether of bisphenol A epoxy; Triethylenetetraminehardener | Fullerene $C_{60}$ | Ultrasonic technique; curing | Tensile strength and elastic modulus increase, by 23 and 46%, respectively; fracture toughness and strain energy release rates improve, by 101 and 85 %, correspondingly | [44] |
| Diglycidyl ether of bisphenol A epoxy; commercial hardener | Fullerene $C_{60}$ | Solution route; sonication; curing | Microstructure with aggregated polymer domains and scattered fullerene nanoparticles; Young's modulus and ultimate tensile strength increase, by 19 and 20 %, respectively | [45] |
| Polyaniline | Fullerene $C_{60}$ | Liquid crystal cells of S-type having initial planar orientation | Complex formation; nematic liquid crystal generation | [56] |
| Polyaniline | Fullerene $C_{60}$ | In situ method | Electron donor-acceptor linkings | [57] |
| Polyaniline emeraldine base | Fullerene $C_{60}$ nanowhiskers | In situ method | Electrostatic interactions; symmetrical triangular galvanostatic charge-discharge curves; optimum capacity; reversible electrochemical profile; specific capacitance 813 $Fg^{-1;}$ capacitance retention > 85 % (1500 cycles) | [59] |
| Polypyrrole | Fullerene $C_{60}$ | In situ oxidation method | Fullerene nanoparticles with diameter, of 500 nm, and band gap, of 0.25 eV | [66] |
| Poly(3-hexylthiophene) | Fullerene $C_{60}$ | Solution route | Hydrogen bonding between fullerene (amine functionalities) and matrix (carbonyl functionalities) | [74] |
| Bisphenol A epoxy; diethylenetrimine curing agent | Fullerene $C_{60}$ | Solution/curing routes | Tafel polarization/Bode plots; anticorrosion potential | [87] |
| Bisphenol A epoxy | Fullerene $C_{60}$-isobenzofulven | Solution/mixing techniques | Bulk heterojunction solar cell; power conversion efficiency 3.1 % open circuit voltage 0.75 V | [94] |
| Poly(3-hexylthiophene)/phenyl-C61-butyric acid methyl ester | Fullerene $C_{60}$- | Solution route | Photovoltaic system; photo conversion efficiency 30 % | [98] |
| Polyaniline | Fullerene plasma-induced carbon clusters | Solution route | Battery photoelectrode; capacity 310 mAh $g^{-1}$; capacity retention 91 % (2000 cycles); photon energy conversion, of 1.15 % | [101] |

Besides, in case of any processing technique, using functional fullerene (e.g., carboxylic acid, hydroxyl, amine) can easily develop better hydrogen bonding and electrostatic interactions with epoxy. In the case of non-functional fullerene, using sonication, magnetic stirring, etc., can enhance interactions between polymer chains and nanoparticles, especially via π-π stacking and van der Waals association. In this way, nanocomposite synthesis technique, additional nanoparticle modification and dispersion assisting techniques may affect the performance of non-covalently linked polymer/fullerene nanocomposites.

***Table 3.*** *Comparison of essential features and technical performance of polymer/fullerene nanocomposites with graphene (two dimensional) and carbon nanotube (one dimensional) derived nanocomposites*

| Matrix | Nano-additive | Fabrication | Features | Ref. |
|---|---|---|---|---|
| Diglycidyl ether of bisphenol A epoxy; Triethylenetetraminehardener | Fullerene $C_{60}$ | Ultrasonic technique; curing | Tensile strength and elastic modulus increased by 23 and 46%, respectively; fracture toughness and strain energy release rates improve, by 101 and 85 %, correspondingly | [44] |
| Diglycidyl ether of bisphenol A epoxy; commercial hardener | Fullerene $C_{60}$ | Solution route; sonication; Curing | Young's modulus and ultimate tensile strength increased by 19 and 20 %, respectively | [45] |
| Diglycidyl ether of bisphenol A epoxy; EPIKURE curing agent W | Graphene nanoplatelets | Curing method | Tensile strength and modulus increased by ~ 8 % and ~ 7 %, respectively | [112] |
| Diglycidyl ether of bisphenol A epoxy; curing agent W | Graphene nanoplatelets | Curing method | Tensile modulus increased by ~ 14 % | [113] |
| Araldite LY-556 epoxy; commercial hardener HY-917 | Carbon nanotube | Curing route | Modified Halpin-Tsai micro-mechanical model based tensile modulus enhanced by 27 % | [114] |
| Bisphenol A epoxy | Fullerene $C_{60}$-isobenzofulven | Solution/mixing techniques | Bulk heterojunction solar cell; power conversion efficiency 3.1 % open circuit voltage 0.75 V | [94] |
| Bisphenol A epoxy | Graphene- | - | Not reported yet. | - |
| Bisphenol A epoxy | Carbon nanotube | - | Not reported yet. | - |
| Poly(3-hexylthiophene)/phenyl-C61-butyric acid methyl ester | Fullerene $C_{60}$- | Solution route | Photovoltaic system; photo conversion efficiency 30 % | [98] |
| Poly(3-hexylthiophene)/phenyl-C61-butyric acid methyl ester | Reduced graphene oxide | Solution route | Bulk heterojunction solar cell; power conversion efficiency ~ 3.9 % | [115] |
| Poly(3-hexylthiophene)/phenyl-C61-butyric acid methyl ester | Carbon nanotube | Spray coating | Photovoltaic system; power conversion efficiency ~ 7 % | [116] |

| | | | | |
|---|---|---|---|---|
| Poly(3-hexylthiophene)/phenyl-C61-butyric acid methyl ester | Boron doped carbon nanotube | Solution route | Bulk heterojunction solar cell; power conversion efficiency ~ 4 % | [117] |
| Polyaniline emeraldine base | Fullerene $C_{60}$ nanowhiskers | In situ route | Electrochemical properties; specific capacitance > 800 $Fg^{-1}$; capacitance retention > 85 % (1500 cycles) | [59] |
| Polyaniline | Graphene | In situ route | Specific capacitance > 300 $Fg^{-1}$; capacitance retention ~ 88 % (1000 cycles) | [118] |
| Polyaniline | Reduced graphene oxide | In situ route | Specific capacitance > 400 $Fg^{-1}$; capacitance retention ~ 84 % (800 cycles) | [119] |
| Polyaniline | Carbon nanotube | In situ chemical oxidation process | Core shell hybrids; specific capacitance > 480 $Fg^{-1}$; capacitance retention ~ 98 % (> 1000 cycles) | [120] |
| Polyaniline | Fullerene plasma-induced carbon clusters | Solution route | Battery electrode; capacity > 300 mAh $g^{-1}$; capacity retention 91 % over 2000 cycles | [101] |
| Polyaniline | Graphene | Ball milling method | Battery anode; capacity ~ 250 mAh $g^{-1}$; capacity retention over 350 cycles | [121] |
| Polyaniline | Carbon nanotube | Carbonization | Battery anode; capacity ~ 260 mAh $g^{-1}$; capacity retention over 150 cycles | [122] |

As presented above, potential of polymer/fullerene nanocomposites have been discovered for corrosion resisting coatings, batteries, supercapacitors, photovoltaics, and allied methodological devices. However, number of design, synthesis, and essential characteristics related challenges need to be resolved to attain high-tech industrial scale fullerene based nanostructures and applications. Broadly speaking, miscibility and dispersion of fullerene molecules in matrices remain as major challenges thru the nanocomposite fabrication. Lack of fullerene solubility/scattering may lead to agglomeration in polymeric matrices. Consequently, poor fullerene dispersion strongly affects physical interaction between matrix-nanofiller and aggregation tendencies. Herein, minute variations in fullerene surface functionalization may enhance *(i)* nanoscale/interfacial miscibility of polymers-fullerenes; *(ii)* interconnectivity of polymer chains-fullerene molecules and fullerene-fullerene; *(iii)* better percolation effects for charge, electron, and ionic transportation. Additionally, challenges have been analyzed to attain sustainability, ecofriendliness, reproducibility, low cost, as well as commercialization in polymer/fullerene hybrids. Hence, using appropriate surface functionalities not only enhance fullerene miscibility but also long-term environmental compatibility.

Correspondingly, future opportunities of thermosetting/fullerene and conjugated polymer/fullerene nanocomposites rely on several factors including facile processing, consistent dispersion, interfacial establishment, and scalability for related industries. Various energy devices based technological fields, such as fuel cells, have yet not been sufficiently explored using these fullerene derived nanocomposites [123]. Predominantly, conductive polymer/fullerene must be focused for electronics, like sensors/actuators [124, 125]. Similarly, research expansions on these nanomaterials efforts may lead to advanced transistor designs [126]. However, the fields of sensors, actuators, transistors, etc. demand extensive

focused future research efforts. Moreover, using fullerene reinforced thermosets or conjugated matrices may benefit the arenas of aerospace and automotive sectors [127]. Furthermore, fullerene derived nanocomposites must be scrutinized for future biomedical fields [128]. Hardly any successful research endeavors seen regarding controlled uptake and release of drugs, thereby making an open field for functional fullerene hybrids based future drug delivery industries [129]. Several biocompatible fullerene based systems can be research for future nanomedicine application [130]. Henceforth, future design and practical opportunities of polymer/fullerene nanocomposites rely upon explorations and inventions of underlying mechanisms for interactions, dispersion, interfaces, and competent physical profiles.

Briefly speaking, it is recommended that comprehensive future research efforts seemed indispensable to overcome the design-processing-property challenges of the physically interlinked polymer/fullerene nanomaterials in order to unveil the myriad of unexplored technological zones, like fuel cells, supercapacitors, optical devices, sensors, microelectronics, *e*-textiles, defence and biomedical applications. Moreover, it can be suggested that according to prior literature surveys hitherto, appropriate surface alterations of fullerene nanoparticles need to be investigated to resolve the challenges of macromolecular/nanofiller agglomeration via developing efficient electrostatic, hydrogen bindings or aromatic stacking interactions, so leading towards advanced property-performance profiles of the high tech polymer/fullerene nanocomposites [131].

Conclusively, this revolutionary overview, well-summarized the current state of the physically or non-covalently interlinked thermosets/fullerene and the conductive/fullerene nanocomposites. In accordance with the literature survey, physical or non-covalent associations between the macromolecular matrix-nanoparticles valuably influenced the microstructural, electron/charge/thermal conductivity, mechanical/heat stability, corrosion resistance, specific capacitance/capacity and photovoltaic properties of the advanced polymer/fullerene nanomaterials. Various simplistic synthesis practices, like in situ, solution and ultrasonication methods, have been applied for the fabrication of the thermosetting matrix/fullerene and the conjugated polymer/fullerene nanocomposites having non-covalent interactions in their nanostructures. In this concern, numerous factors seem to influence the polymer/fullerene nanocomposite characteristics, including type and molecular weight of the macromolecular matrix, solubility properties of the macromolecular matrix, fullerene contents, fullerene surface modification, scattering patterns of macromolecules and/or nanoparticles, interfacial linkages and processing technique used for the formation of these hybrids. Subsequently, the polymer/fullerene nanocomposites having physical interaction between their macromolecular matrix-nanofiller phases have been explored for their application in corrosion defense and energy devices/systems. Henceforth, despite the non-covalently interlinked polymer/fullerene based technical systems reported thus far, upcoming research endeavors must focus the development of innovative macromolecular-nanofiller design combinations and invention/use of advanced processing methods to resolve the design-synthesis-property challenges in order to attain future high-tech fullerene reinforced thermosetting and conducting macromolecular hybrid systems for real world industrial applications.

## REFERENCES


1. Xue, S., et al., *Simultaneous reinforcement and toughening of thermosets and its mechanism: a review.* Materials Horizons, 2025.
2. Musa, A.A., et al., *Nano-enhanced polymer composite materials: a review of current advancements and challenges.* Polymers, 2025. 17(7): p. 893.
3. Ujah, C.O. and P.A. Olubambi, *Exploring New Potential Applications of Carbon Nanomaterials Through Simulation.* Advances in Materials Science and Engineering, 2025. 2025(1): p. 9216747.
4. Huang, J., et al., *Anti-corrosive and UV-resistant three-dimensional epoxy coating based on reduced graphene oxide, modified carbon nanotubes, modified fullerene, and 2-(2'-hydroxy-5'-methylphenyl) benzotriazole for polycarbonate/acrylonitrile-styrene-acrylic.* Polymer Degradation and Stability, 2024. 220: p. 110629.
5. Akhanova, N.Y., et al., *Influence of Fullerene Content on the Properties of Polyurethane Resins: A Study of Rheology and Thermal Characteristics.* Heliyon, 2024.
6. Rayar, A., et al., *Organic conjugated polymers and their nanostructured composites: Synthesis methodologies and electrochemical applications.* Nano-Structures & Nano-Objects, 2024. 37: p. 101102.
7. Hasan, M.B., et al., *A review on conducting organic polymers: Concepts, applications, and potential environmental benefits.* Heliyon, 2025. 11(3).
8. Samoilova, N.A., et al., *Hydrophilization and Functionalization of Fullerene C60 with Maleic Acid Copolymers by Forming a Non-Covalent Complex.* Polymers, 2024. 16(12): p. 1736.
9. Lu, J., et al., *Non-covalent Intramolecular Interactions Induced High-Performance Terpolymer Donors.* Advanced Functional Materials, 2024. 34(13): p. 2312545.
10. Harris, P.J., *Fullerene polymers: A brief review.* C, 2020. 6(4): p. 71.
11. Panda, J., et al., *Fullerenes: Synthesis and Applications*, in *New Forms of Carbon*. 2024, Apple Academic Press. p. 93-122.
12. Kurniawan, D., et al., *Zero-dimensional nano-carbons: Synthesis, properties, and applications.* Applied Physics Reviews, 2024. 11(2).
13. Wössner, J.S., et al., *[n] Cyclodibenzopentalenes as Antiaromatic Curved Nanocarbons with High Strain and Strong Fullerene Binding.* Journal of the American Chemical Society, 2021. 143(31): p. 12244-12252.
14. Buseck, P.R., S.J. Tsipursky, and R. Hettich, *Fullerenes from the geological environment.* Science, 1992. 257(5067): p. 215-217.
15. Ito, K., et al., *An aromatic micelle with bent pentacene-based panels: encapsulation of perylene bisimide dyes and graphene nanosheets.* Chemical science, 2020. 11(26): p. 6752-6757.
16. Kulkarni, K., et al., *A review on the smallest carbon fullerene C20: Applications and device formation.* Materials Today: Proceedings, 2024.
17. 17. Jaiswal, S., S. Tiwari, and P.S. Bahadur, *Inter-stellar Space Discovery, Spectroscopic Structure identification and Application of C60 Buckminsterfullerene.* Int. J. Eng. Res. Gen. Sci, 2021. 9: p. 12-19.
18. David, A.H., et al., *Heptagon-Containing Saddle-Shaped Nanographenes: Self-Association and Complexation Studies with Polycyclic Aromatic Hydrocarbons and Fullerenes.* Organic Materials, 2021. 3(01): p. 051-059.

19. Ghavanloo, E., et al., *Experimental and computational physics of fullerenes and their nanocomposites: Synthesis, thermo-mechanical characteristics and nanomedicine applications.* Physics Reports, 2023. 996: p. 1-116.
20. Paukov, M., et al., *Functionalized fullerenes and their applications in electrochemistry, solar cells, and nanoelectronics.* Materials, 2023. 16(3): p. 1276.
21. Danilenko, V.V., *On the discovery of detonation nanodiamond*, in *Ultrananocrystalline Diamond*. 2006, Elsevier. p. 335-345.
22. Kroto, H.W., et al., *C60: Buckminsterfullerene.* nature, 1985. 318(6042): p. 162-163.
23. Ugarte, D., *Curling and closure of graphitic networks under electron-beam irradiation.* Nature, 1992. 359(6397): p. 707-709.
24. Xu, X., et al., *Electrophoretic analysis and purification of fluorescent single-walled carbon nanotube fragments.* Journal of the American Chemical Society, 2004. 126(40): p. 12736-12737.
25. Devika, V., et al., *Applications of zero-dimensional carbon–based nanomaterials as optical and electrochemical sensors*, in *Zero-Dimensional Carbon Nanomaterials*. 2024, Elsevier. p. 497-514.
26. Tang, C., et al., *A Geometrically Flexible Three-Dimensional Nanocarbon.* Journal of the American Chemical Society, 2024.
27. Wang, Y., G.J. Desroches, and R.J. Macfarlane, *Ordered polymer composite materials: challenges and opportunities.* Nanoscale, 2021. 13(2): p. 426-443.
28. Latif, Z., et al., *Thermal and mechanical properties of nano-carbon-reinforced polymeric nanocomposites: A review.* Journal of Composites Science, 2023. 7(10): p. 441.
29. Adem, A.A., H. Panjiar, and B. Daniel, *Analysis of Nanocarbon Effect on Polymer Composite Tribological Properties.* Journal of Engineering Science & Technology Review, 2024. 17(2).
30. Dhanushree, S. and C. Nithya, *Introduction to Nanocarbon*, in *NanoCarbon: A Wonder Material for Energy Applications: Volume 1: Basics to Advanced Applications for Energy Production*. 2024, Springer. p. 1-15.
31. Artyukov, I., et al., *Studies of Fractal Microstructure in Nanocarbon Polymer Composites.* Polymers, 2024. 16(10): p. 1354.
32. Vejpravová, J., *Mixed sp2–sp3 nanocarbon materials: a status quo review.* Nanomaterials, 2021. 11(10): p. 2469.
33. Kinloch, I.A., et al., *Composites with carbon nanotubes and graphene: An outlook.* Science, 2018. 362(6414): p. 547-553.
34. Mu, J., et al., *Influence mechanism of dispersion and agglomeration characteristics of micron/nano carbon dust on its combustion kinetics and explosion process.* Fullerenes, Nanotubes and Carbon Nanostructures, 2024. 32(2): p. 165-182.
35. Adem, A.A., H. Panjiar, and B.S.S. Daniel, *The effect of nanocarbon inclusion on mechanical, tribological, and thermal properties of phenolic resin-based composites: An overview.* Engineering Reports, 2024. 6(4): p. e12861.
36. Dinu, R., et al., *New Generation of Recyclable High-Performance Biobased Epoxy Thermosets and Composites.* ACS Sustainable Chemistry & Engineering, 2024.
37. Xiang, Q. and F. Xiao, *Applications of epoxy materials in pavement engineering.* Construction and Building Materials, 2020. 235: p. 117529.

38. Taylor, O., et al., *Characterization of the Mechanical and Thermal Properties, Including Fracture Toughness, of Epoxy Resin System DGEBA, POPDA (D400).* IEEE Transactions on Applied Superconductivity, 2024.

39. Xing, A., et al., *A trifunctional active ester for curing DGEBA: synthesis, curing behavior, and properties of its cured product.* Journal of Polymer Research, 2024. 31(3): p. 66.

40. Gangil, B., et al., *Introduction to thermosetting polymer composites: applications, advantages, and drawbacks*, in *Dynamic Mechanical and Creep-Recovery Behavior of Polymer-Based Composites*. 2024, Elsevier. p. 11-19.

41. Thamizh Selvan, R., et al., *Recycling technology of epoxy glass fiber and epoxy carbon fiber composites used in aerospace vehicles.* Journal of Composite Materials, 2021: p. 00219983211011532.

42. Esmail, R., et al., *Effect of presence of SWCNT and Fullerene nano particles in the adhesive of CFRP single lap joint on the lap shear strength subjected to hygrothermal conditions.* Journal of Adhesion Science and Technology, 2023. 37(21): p. 3013-3029.

43. Xiang, Y., L. Li, and S. Zheng, *Morphologies and dielectric properties of epoxy thermosets containing poly (N-vinylcarbazole), fullerene-C60 and their charge transfer complex nanophases.* Polymer, 2018. 138: p. 113-123.

44. Das, S., S. Halder, and N.I. Khan, *Mechanical properties of oxidized fullerene C60/epoxy nanocomposite.* Materials Today: Proceedings, 2019. 18: p. 655-659.

45. Rafiee, M.A., et al., *Fullerene–epoxy nanocomposites-enhanced mechanical properties at low nanofiller loading.* Journal of Nanoparticle Research, 2011. 13(2): p. 733-737.

46. Rodríguez-Martínez, X., et al., *On The Thermal Conductivity of Conjugated Polymers for Thermoelectrics.* Advanced Energy Materials, 2024: p. 2401705.

47. Pilo, M.I., G. Sanna, and N. Spano, *Conducting Polymers in Amperometric Sensors: A State of the Art over the Last 15 Years with a Focus on Polypyrrole-, Polythiophene-, and Poly (3, 4-ethylenedioxythiophene)-Based Materials.* Chemosensors, 2024. 12(5): p. 81.

48. Dua, S., et al., *Conjugated polymer-based composites for anti-corrosion applications.* Progress in Organic Coatings, 2024. 188: p. 108231.

49. Paleti, S.H.K., et al., *Impact of doping on the mechanical properties of conjugated polymers.* Chemical Society Reviews, 2024.

50. Qiu, Z., B.A. Hammer, and K. Müllen, *Conjugated polymers–Problems and promises.* Progress in Polymer Science, 2020. 100: p. 101179.

51. Wei, H., et al., *Multifunctions of polymer nanocomposites: environmental remediation, electromagnetic interference shielding, and sensing applications.* ChemNanoMat, 2020. 6(2): p. 174-184.

52. Kazemi, F., et al., *Biosensing applications of polyaniline (PANI)-based nanocomposites: a review.* Polymer Reviews, 2021. 61(3): p. 553-597.

53. Riaz, U., et al., *A review on synthesis and applications of polyaniline and polypyrrole hydrogels.* Polymer Bulletin, 2023. 80(2): p. 1085-1116.

54. Kandpal, R., et al., *Polyaniline-Based Flexible Nanocomposite Materials*, in *Biorenewable Nanocomposite Materials, Vol. 1: Electrocatalysts and Energy Storage*. 2022, ACS Publications. p. 367-395.

55. Shubhadarshinee, L., et al., *Review on synthesis and characterization of metal nanoparticles doped carbon nanofillers based nanohybrids reinforced polyaniline nanocomposites.* Polymer-Plastics Technology and Materials, 2024. 63(8): p. 1011-1035.

56. Zubtsova, Y.A., et al., *Study of Dynamic and Nonlinear Optical Properties of Polyaniline–Fullerene–Liquid Crystal Structures.* Molecular Crystals and Liquid Crystals, 2007. 467(1): p. 171-180.
57. Xiong, S., et al., *Covalently bonded polyaniline/fullerene hybrids with coral-like morphology for high-performance supercapacitor.* Electrochimica acta, 2012. 85: p. 235-242.
58. Mathew, R.J., et al., *Tuning of nonlinear optical bistability tuned by fullerene concentration in polyaniline-fullerene (PANI-C60) hybrid organic films.* Next Nanotechnology, 2025. 8: p. 100236.
59. Wang, H., X. Yan, and G. Piao, *A high-performance supercapacitor based on fullerene C60 whisker and polyaniline emeraldine base composite.* Electrochimica acta, 2017. 231: p. 264-271.
60. Riaz, M., et al., *Synergistic Electrochemical Performance of PANI and Fullerene (C60) Based Novel Composites with Halide Perovskites (CsInCl3) for Advanced Supercapacitors Electrodes.* Journal of Inorganic and Organometallic Polymers and Materials, 2025. 35(3): p. 1891-1899.
61. Halium, E.M., et al., *High-performance one and two-dimensional doped polypyrrole nanostructure for polymer solar cells applications.* Journal of Materials Science: Materials in Electronics, 2022. 33(13): p. 10165-10182.
62. Sood, Y., et al., *Insights into properties, synthesis and emerging applications of polypyrrole-based composites, and future prospective: A review.* Heliyon, 2024.
63. Mahmood, J., et al., *Preparation and characterization of hybrid polypyrrole nanoparticles as a conducting polymer with controllable size.* Scientific Reports, 2024. 14(1): p. 11653.
64. Thummarungsan, N., D. Pattavarakorn, and A. Sirivat, *Electrically responsive materials based on dibutyl phathalate plasticized poly (lactic acid) and spherical fullerene.* Smart Materials and Structures, 2022. 31(3): p. 035029.
65. Zhou, F.F., et al. *Effects of Phosphoric Acid on the Photovoltaic Properties of Photovoltaic Cells with Laminated Polypyrrole-Fullerene Layers*. in *Materials Science Forum*. 2011. Trans Tech Publ.
66. Wysocka-Zolopa, M., et al., *Polypyrrole nanoparticles doped with fullerene uniformly distributed in the polymeric phase: synthesis, morphology, and electrochemical properties.* The Journal of Physical Chemistry C, 2018. 122(44): p. 25539-25554.
67. Wang, J., et al., *The construction of carbon nanofiber composites modified by graphene/polypyrrole for flexible supercapacitors.* Journal of Energy Storage, 2022. 51: p. 104581.
68. Nandi, A.K., *A Review on Self-Assembly Driven Optoelectronic Properties of Polythiophene-Peptide and Polythiophene-Polymer Conjugates.* Langmuir, 2024. 40(18): p. 9385-9405.
69. Hassan, A., et al., *Effect of heteroatoms on structural, electronic and spectroscopic properties of polyfuran, polythiophene and polypyrrole: A hybrid DFT approach.* Journal of Molecular Structure, 2023. 1274: p. 134484.
70. An, M., et al., *Polythiophene Derivatives for Efficient All-Polymer Solar Cells.* Advanced Energy Materials, 2023. 13(30): p. 2301110.
71. AL-Refai, H.H., A.A. Ganash, and M.A. Hussein, *Polythiophene and its derivatives–Based nanocomposites in electrochemical sensing: A mini review.* Materials Today Communications, 2021. 26: p. 101935.
72. Kassem, H., A. Salehi, and M. Kahrizi, *Recent Advances in Poly (3-hexylthiophene) and Its Applications in Perovskite Solar Cells.* Energy Technology, 2024. 12(5): p. 2301032.

73. Elashry, M., et al., *An investigation of structural, optical, and electrical properties of poly (3-hexylthiophene)/reduced graphene oxide nanocomposites for electronic and optoelectronic applications.* Polymers for Advanced Technologies, 2024. 35(1): p. e6220.

74. Li, F., et al., *Conjugated polymer/fullerene nanostructures through cooperative non-covalent interactions for organic solar cells.* Polymer, 2015. 76: p. 220-229.

75. Kumar, G.P., et al., *Concentration driven changes in structural, optical, and electrochemical properties of spin coated poly 3-hexylthiophene (P3HT) thin films via fullerene (C60) incorporation.* Materials Science and Engineering: B, 2026. 323: p. 118834.

76. Räder, J., C. Cocchi, and M. Guerrini, *Laser-Driven Charge-Transfer Dynamics in the Quaterthiophene–Fullerene Donor/Acceptor Interface.* ChemPhotoChem, 2025. 9(11): p. e202500116.

77. Rasheed, M.H., et al., *Electrochemically Tailored Polythiophene–Fullerene Heterostructures Integrated with Binary-Cation Modulated Quasi-Solid-State Ionic Gel Electrolytes for Enhanced Interfacial Kinetics in Dye-Sensitized Solar Cells.* Synthetic Metals, 2026: p. 118074.

78. Mahmoud, A.Y., *Annealing and thickness dependent enhanced-efficiency of P3HT: PCBM organic solar cells.* Energy Exploration & Exploitation, 2026: p. 01445987251413622.

79. Kakogianni, S., A.K. Andreopoulou, and J.K. Kallitsis, *Synthesis of Polythiophene–Fullerene Hybrid Additives as Potential Compatibilizers of BHJ Active Layers.* Polymers, 2016. 8(12): p. 440.

80. Kitao, T., et al., *Selective Formation of End-on Orientation between Polythiophene and Fullerene Mediated by Coordination Nanospaces.* The Journal of Physical Chemistry C, 2018. 122(42): p. 24182-24189.

81. Gobara, M., et al., *Corrosion protection mechanism of Ce 4+/organic inhibitor for AA2024 in 3.5% NaCl.* RSC Advances, 2020. 10(4): p. 2227-2240.

82. Wang, J., et al., *The effects of temperature and alignment state of nanofillers on the thermal conductivity of both metal and nonmetal based graphene nanocomposites.* Acta Materialia, 2020. 185: p. 461-473.

83. Boppana, S.B., et al., *Synthesis and characterization of nano graphene and ZrO2 reinforced Al 6061 metal matrix composites.* Journal of Materials Research and Technology, 2020. 9(4): p. 7354-7362.

84. Turan, M.E., et al., *Effects of carbonaceous reinforcements on microstructure and corrosion properties of magnesium matrix composites.* Materials Chemistry and Physics, 2018. 218: p. 182-188.

85. Samadianfard, R., et al., *Oxidized fullerene/sol-gel nanocomposite for corrosion protection of AM60B magnesium alloy.* Surface and Coatings Technology, 2020. 385: p. 125400.

86. Shukla, M. and S. Kumar, *Carbon allotropes in corrosion prevention: Computational-based advancements*, in *Carbon Allotropes*. 2024, CRC Press. p. 167-179.

87. Liu, D., et al., *Comparative tribological and corrosion resistance properties of epoxy composite coatings reinforced with functionalized fullerene C60 and graphene.* Surface and Coatings Technology, 2016. 286: p. 354-364.

88. Verma, D.K., E. Berdimurodov, and F. Khan, *Advanced Anti-Corrosive Materials*. 2026: CRC Press.

89. Babahan Bircan, I., et al., *Improving Surface Properties of Wood Material Against Weathering by Using New Bio-based Epoxy Nanocomposites.* Drvna industrija, 2025. 76(3): p. 317-330.

90. Yan, L. and C.-Q. Ma, *Degradation of polymer solar cells: knowledge learned from the polymer: fullerene solar cells.* Energy Technology, 2021. 9(4): p. 2000920.

91. Lin, K., et al., *Novel cross-linked films from epoxy-functionalized conjugated polymer and amine based small molecule for the interface engineering of high-efficiency inverted polymer solar cells.* Solar Energy Materials and Solar Cells, 2017. 168: p. 22-29.
92. Mumyatov, A.V. and P.A. Troshin, *A review on fullerene derivatives with reduced electron affinity as acceptor materials for organic solar cells.* Energies, 2023. 16(4): p. 1924.
93. Han, G.D., et al., *Cyclobutadiene–C60 Adducts: N-Type Materials for Organic Photovoltaic Cells with High VOC.* Advanced Functional Materials, 2013. 23(24): p. 3061-3069.
94. Han, G.D., et al., *VOC enhancement in polymer solar cells with isobenzofulvene–C60 adducts.* Organic Electronics, 2016. 31: p. 48-55.
95. Chen, Y.-P., S. Bashir, and J.L. Liu, *Nanostructured materials for next-generation energy storage and conversion: hydrogen production, storage, and utilization*. 2017: Springer.
96. Ozturk, S.E., et al., *Synthesis, Photophysical properties and OFET application of thienothiophene and benzothiadiazole based Donor-π-Acceptor-π (D-π-A-π) type conjugated polymers.* European Polymer Journal, 2023. 191: p. 112028.
97. Ma, L., et al., *Morphology control by tuning electrostatic interactions for efficient polythiophene-based all-polymer solar cells.* Chem, 2023. 9(9): p. 2518-2529.
98. Lobez, J.M., et al., *Improving the performance of P3HT–fullerene solar cells with side-chain-functionalized poly (thiophene) additives: a new paradigm for polymer design.* ACS nano, 2012. 6(4): p. 3044-3056.
99. Rodríguez-Seco, C., et al., *Photoactive nanomaterials enabled integrated photo-rechargeable batteries.* Nanophotonics, 2022. 11(8): p. 1443-1484.
100. Zhang, M., et al., *Multiplying Light Harvest Driven by Hybrid-Reflections 3D Electrodes Achieves High-Availability Photo-Charging Zinc-Ion Batteries.* Advanced Energy Materials, 2023. 13(15): p. 2204058.
101. Tran, M.X., et al., *A flexible fiber-shaped solar chargeable zinc–polyaniline battery with a fullerene-based electron transfer layer.* Energy Storage Materials, 2024. 65: p. 103145.
102. Huang, X., et al., *Efficient oxygen reduction catalysts of porous carbon nanostructures decorated with transition metal species.* Advanced Energy Materials, 2020. 10(11): p. 1900375.
103. Haque, A., et al., *Non-covalent interactions (NCIs) in π-conjugated functional materials: advances and perspectives.* Chemical Society Reviews, 2023. 52(2): p. 454-472.
104. Ortiz-Soto, K.A., et al., *Charge Transfer in Self-Assembled Fullerene-Tetraphenylporphyrin Non-Covalent Multilayer.* ECS Journal of Solid State Science and Technology, 2022. 11(1): p. 014001.
105. Boumeftah, A., A. Belmokhtar, and A. Benyoucef, *Polymer/Carbon Nanocomposites: Synthesis, Properties and Application in Solar Energy*, in *Advances in Nanocomposite Materials for Environmental and Energy Harvesting Applications*. 2022, Springer. p. 795-816.
106. Grądzka, E., M. Wysocka-Żołopa, and K. Winkler, *Fullerene-Based Conducting Polymers: n-Dopable Materials for Charge Storage Application.* Advanced Energy Materials, 2020. 10(40): p. 2001443.
107. PAYYAPPILLY, S.S., *Polythiophene Nanocomposites and their Applications.* Functional Nanocomposites and Their Applications, 2024: p. 27.
108. Phor, L., A. Kumar, and S. Chahal, *Electrode materials for supercapacitors: a comprehensive review of advancements and performance.* Journal of Energy Storage, 2024. 84: p. 110698.
109. Gizdavic-Nikolaidis, M., et al., *Rapid microwave synthesis of polyaniline–C60 nanocomposites.* Synthetic Metals, 2016. 217: p. 14-18.

110. Choudhary, R.B., S. Ansari, and B. Purty, *Robust electrochemical performance of polypyrrole (PPy) and polyindole (PIn) based hybrid electrode materials for supercapacitor application: A review.* Journal of Energy Storage, 2020. 29: p. 101302.

111. Oh, S.M., C.H. Lee, and S.Y. Kim, *Processing method determines the long-term stability of particle dispersions in concentrated nanoparticle/polymer suspensions.* Soft Matter, 2022. 18(4): p. 841-848.

112. Klimek-McDonald, D.R., et al., *Determination and modeling of mechanical properties for graphene nanoplatelet/epoxy composites.* Polymer Composites, 2018. 39(6): p. 1845-1851.

113. King, J.A., et al., *Mechanical properties of graphene nanoplatelet/epoxy composites.* Journal of Composite Materials, 2015. 49(6): p. 659-668.

114. Srivastava, V.K., *Modeling and mechanical performance of carbon nanotube/epoxy resin composites.* Materials & Design, 2012. 39: p. 432-436.

115. Qu, S., et al., *Noncovalent functionalization of graphene attaching [6, 6]-phenyl-C61-butyric acid methyl ester (PCBM) and application as electron extraction layer of polymer solar cells.* Acs Nano, 2013. 7(5): p. 4070-4081.

116. Kumar, A., et al., *Spray deposited carbon nanotube embedded ZnO as an electrons transport layer in inverted organic solar cells.* Hybrid Advances, 2023. 4: p. 100088.

117. Lee, J.M., et al., *Selective electron-or hole-transport enhancement in bulk-heterojunction organic solar cells with N-or B-doped carbon nanotubes.* Advanced Materials, 2011. 23(5): p. 629-633.

118. Ates, M., M. El-Kady, and R.B. Kaner, *Three-dimensional design and fabrication of reduced graphene oxide/polyaniline composite hydrogel electrodes for high performance electrochemical supercapacitors.* Nanotechnology, 2018. 29(17): p. 175402.

119. Wang, Y., et al., *Facile route for the preparation of functionalized reduced graphene oxide/polyaniline composite and its enhanced electrochemical performance.* ECS Journal of Solid State Science and Technology, 2021. 10(3): p. 031003.

120. Thanasamy, D., et al., *Microstructural effect of various polyaniline-carbon nanotube core-shell nanocomposites on electrochemical supercapacitor electrode performance.* Journal of Energy Storage, 2022. 53: p. 105087.

121. Fu, H., et al., *Graphene nanonetwork embedded with polyaniline nanoparticles as anode of Li-ion battery.* Chemical Engineering Journal, 2023. 477: p. 146936.

122. Tian, S., et al., *Polyaniline-derived carbon nanotubes as anode materials for potassium-ion batteries: Insight into the effect of N-doping.* Applied Surface Science, 2020. 534: p. 147635.

123. Hernández-Herrera, C., et al., *Numerical Assessment of Heat Transfer on a PEM Fuel Cell Stack with Different Refrigeration Systems: Heat Source Management.* Int. J. Electrochem. Sci, 2022. 17(220554): p. 2.

124. Pavel, I.-A., S. Lakard, and B. Lakard, *Flexible Sensors Based on Conductive Polymers.* Chemosensors, 2022. 10(3): p. 97.

125. Wang, C.-C., S.-C. Wei, and S.-C. Luo, *Recent advances and biomedical applications of peptide-integrated conducting polymers.* ACS Applied Bio Materials, 2022.

126. Nosho, Y., et al., *n-type carbon nanotube field-effect transistors fabricated by using Ca contact electrodes.* Applied Physics Letters, 2005. 86(7): p. 073105.

127. Kausar, A., *Advances in condensation polymer containing zero-dimensional nanocarbon reinforcement—fullerene, carbon nano-onion, and nanodiamond.* Polymer-Plastics Technology and Materials, 2021. 60(7): p. 695-713.

128. Pochkaeva, E.I., et al., *Fullerene derivatives with amino acids, peptides and proteins: From synthesis to biomedical application.* Progress in Solid State Chemistry, 2020. 57: p. 100255.

129. Alipour, E., et al., *Fullerene C60 containing porphyrin-like metal center as drug delivery system for ibuprofen drug.* Journal of Molecular Modeling, 2020. 26(1): p. 1-8.

130. P Galvan, Y., et al., *Fullerenes as anti-aging antioxidants.* Current aging science, 2017. 10(1): p. 56-67.

131. Fazio, E., A. Ridolfo, and G. Neri, *Thermally Activated Noble Metal Nanoparticles Incorporated in Electrospun Fiber-based Drug Delivery Systems.* Current Nanomaterials, 2019. 4(1): p. 21-31.